NASA TECHNICAL NOTE

NASA TN D-8120

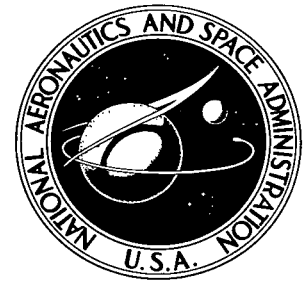

NASA TN D-8120

INFLUENCE OF PARTICLE DRAG COEFFICIENT ON PARTICLE MOTION IN HIGH-SPEED FLOW WITH TYPICAL LASER VELOCIMETER APPLICATIONS

Michael J. Walsh

Langley Research Center
Hampton, Va. 23665

NATIONAL AERONAUTICS AND SPACE ADMINISTRATION • WASHINGTON, D. C. • FEBRUARY 1976

1. Report No.	2. Government Accession No.	3. Recipient's Catalog No.
NASA TN D-8120		

4. Title and Subtitle	5. Report Date
INFLUENCE OF PARTICLE DRAG COEFFICIENT ON PARTICLE MOTION IN HIGH-SPEED FLOW WITH TYPICAL LASER VELOCIMETER APPLICATIONS	February 1976
	6. Performing Organization Code

7. Author(s)	8. Performing Organization Report No.
Michael J. Walsh	L-10258
	10. Work Unit No.
9. Performing Organization Name and Address	505-06-15-01
NASA Langley Research Center Hampton, Va. 23665	11. Contract or Grant No.
	13. Type of Report and Period Covered
12. Sponsoring Agency Name and Address	Technical Note
National Aeronautics and Space Administration Washington, D.C. 20546	14. Sponsoring Agency Code

15. Supplementary Notes

16. Abstract

The effect of using different particle drag coefficient C_D equations for computing the velocity of seeded particles in high-speed gas flows has been investigated. The C_D equations investigated include the Stokes equation, a second incompressible equation valid for higher relative Reynolds numbers, and six more detailed equations that account for the effects of compressibility together with the effects of relative Reynolds numbers greater than one. The flows investigated are center-line nozzle flows, normal shocks, and oblique shocks for free-stream Mach numbers of 1.6 to 6 and stagnation pressures of 1 and 3.4 atmospheres. Particle sizes range from 0.5 to 10 μm. These flows were selected because of their similarity to flows encountered in previous laser velocimeter studies in supersonic flows. The accuracy of the data on which the empirical C_D equations are based was also investigated. The net result is an empirical C_D equation based on the latest sphere C_D data for the low relative Mach number and Reynolds number conditions that are encountered in supersonic flows. This new C_D equation is also used to examine the effect of gas density on the relaxation length behind a Mach 6 normal shock for stagnation pressures from 0.3446 to 20.7 MN/m^2 (3.4 to 204 atm). (1 atmosphere equals 101.3 kN/m^2.)

17. Key Words (Suggested by Author(s))	18. Distribution Statement
Particle drag coefficient Two-phase flow High-speed flow	Unclassified – Unlimited Subject Category 34

19. Security Classif. (of this report)	20. Security Classif. (of this page)	21. No. of Pages	22. Price*
Unclassified	Unclassified	56	$4.25

*For sale by the National Technical Information Service, Springfield, Virginia 22161

INFLUENCE OF PARTICLE DRAG COEFFICIENT ON PARTICLE MOTION IN HIGH-SPEED FLOW WITH TYPICAL LASER VELOCIMETER APPLICATIONS

Michael J. Walsh
Langley Research Center

SUMMARY

The effect of using different particle drag coefficient C_D equations for computing the velocity of seeded particles in high-speed gas flows has been investigated. The C_D equations investigated include the Stokes equation, a second incompressible equation valid for higher relative Reynolds numbers, and six more detailed equations that account for the effects of compressibility together with the effects of relative Reynolds numbers greater than one. The flows investigated are center-line nozzle flows, normal shocks, and oblique shocks for free-stream Mach numbers of 1.6 to 6 and stagnation pressures of 1 and 3.4 atmospheres. Particle sizes range from 0.5 to 10 μm. These flows were selected because of their similarity to flows encountered in previous laser velocimeter studies in supersonic flows. The accuracy of the data on which the empirical C_D equations are based was also investigated. The net result is an empirical C_D equation based on the latest sphere C_D data for the low relative Mach number and Reynolds number conditions that are encountered in supersonic flows. This new C_D equation is also used to examine the effect of gas density on the relaxation length behind a Mach 6 normal shock for stagnation pressures from 0.3446 to 20.7 MN/m^2 (3.4 to 204 atm). (1 atmosphere equals 101.3 kN/m^2.)

INTRODUCTION

The laser velocimeter (LV) is an instrument used to determine flow-field velocities by measuring the velocities of particles seeded in high-speed gas flows. Problems occur in the application of the LV to flows where large velocity gradients are present. The presence of such gradients in many supersonic flows creates a situation where the particles cannot accelerate or decelerate as rapidly as the gas does. The resulting difference between the gas velocity and particle velocity is called the particle "velocity lag." When using an LV system in a supersonic flow, the investigator must consider this particle velocity-lag error.

To measure gas velocity in a supersonic flow, limitation of particle diameters to approximately 1 μm may be necessary to minimize particle velocity lag. However, the Mie scattering criteria (ref. 1) and the characteristics of the LV system (as discussed in ref. 2) may limit the minimum particle size used in an LV application. Thus, particle-motion studies are necessary to determine the size of particles required to follow the gas flow; when the Mie scattering criteria limits the minimum size, these calculations are necessary to determine the particle velocity lag. The particle motion is governed by the flow-field properties, the particle properties, and the particle drag coefficient C_D. A search of the literature in the area of high-speed flows reveals that a number of equations have been used for particle-motion studies, ranging from the simplest Stokes C_D equation (ref. 3) to the more detailed equations of references 4 to 10. To date only two studies have examined the influence of C_D on particle-motion calculations. Maxwell and Seasholtz (ref. 11) used two incompressible C_D equations and the equation of Carlson and Hoglund (ref. 6) to compare the particle-motion calculations behind Mach 1 to Mach 2 normal shocks. In reference 10, Korkan, Petrie, and Bodonyi used the equations of references 4, 6, and 7 to compare particle-motion calculations for uniform flow, Prandtl-Meyer expansions, and oblique shocks in a Mach 5 flow.

The objectives of this investigation are: (1) to determine how well the C_D equations of references 4 to 10 predict the latest available sphere C_D data and, if necessary, to improve the accuracy of sphere C_D "predictions"; (2) to determine the influence of C_D on particle-motion calculations for various high-speed gas flows using the C_D equations of references 4 to 10; and (3) to examine the influence of gas density on particle motion behind a normal shock.

SYMBOLS

C_D drag coefficient

D diameter, μm

M Mach number

N_{Kn} Knudsen number based on particle diameter

$N_{Re,r}$ relative Reynolds number

p pressure, N/m^2

R	specific gas constant, J/kg-K
T	temperature, K
t	time, s
V	velocity, m/s
X	distance, m
γ	ratio of specific heats for gas
θ	percent velocity lag (eq. (14))
λ	relaxation length, distance from shock to point where θ = 1 percent, cm
μ	viscosity, N-s/m^2
ρ	density, 919.5 kg/m^3

Subscripts:

C	continuum
comp	compressible
FM	free molecular
g	gas
inc	incompressible
max	maximum
p	particle
r	relative
x	x-component

y	y-component
0	tunnel stagnation conditions
∞	free stream

An arrow over a symbol represents a vector quantity.

DISCUSSION

Governing Equation for Particle Motion

When applying laser velocimeter (LV) systems to gas flows where particle velocity lag is significant, the motion of the particle becomes important. In these LV applications the particle mass densities are typically much greater than that of the gas. The governing equation for a spherical particle traveling in a fluid where the particle mass density is much greater than the gas density is given by Soo (ref. 3) as

$$\frac{d\vec{V}_p}{dt} = \frac{3}{4} C_D \frac{\rho_g}{\rho_p} \frac{1}{D_p} \left(\vec{V}_g - \vec{V}_p\right) \left|\vec{V}_g - \vec{V}_p\right| \tag{1}$$

By defining a relative Reynolds number based on the velocity difference between the gas and the particle as

$$N_{Re,r} = \frac{\rho_g \left|\vec{V}_g - \vec{V}_p\right| D_p}{\mu_g} \tag{2}$$

equation (1) becomes

$$\frac{d\vec{V}_p}{dt} = \frac{3}{4} \frac{C_D N_{Re,r} \mu_g}{\rho_p D_p^2} \left(\vec{V}_g - \vec{V}_p\right) \tag{3}$$

Thus, the particle acceleration depends on $N_{Re,r}$, flow-field properties, particle mass density, particle size, velocity lag, and C_D.

As discussed in references 4 and 5, equation (3) can be treated in component form for two-dimensional flows as

$$\frac{dV_{p,x}}{dt} = \frac{3}{4} \frac{C_D N_{Re,r} \mu_g (V_{g,x} - V_{p,x})}{\rho_p D_p^2} \tag{4}$$

and

$$\frac{dV_{p,y}}{dt} = \frac{3}{4} \frac{C_D N_{Re,r} \mu_g (V_{g,y} - V_{p,y})}{\rho_p D_p^2} \tag{5}$$

To complete the system of governing differential equations, two additional differential equations are obtained from the definition of velocity:

$$\frac{dX}{dt} p \equiv V_{p,x} \tag{6}$$

$$\frac{dy}{dt} p \equiv V_{p,y} \tag{7}$$

Thus, a numerical solution of equations (4) to (7) gives the particle motion through any known two-dimensional flow field, provided the components of initial particle velocity and position, particle properties, and gas properties are known. Various mathematic representations of the C_D term appearing in equations (4) to (5) are discussed in the following section.

Review of Methods for Calculating C_D

A search of the literature concerning high-speed flows revealed that theoretical solutions for C_D exist only for low relative Reynolds number $(N_{Re,r} < 1)$, incompressible flows, and free-molecular flows. For these $N_{Re,r}$ values the Stokes C_D equation from reference 3

$$C_D = \frac{24}{N_{Re,r}} \tag{8}$$

is valid. For free-molecular flows assuming diffuse reflection, Emmons (ref. 12) gives the following C_D equation:

$$C_{D,FM} = (1 + 2s^2) \exp\left(\frac{-s^2/2}{\sqrt{\pi} s^3}\right) + \frac{(4s^4 + 4s^2 - 1)}{2s^4} \operatorname{erf}(s) + 2\sqrt{\pi} \frac{(T_p/T_g)^{1/2}}{3s} \tag{9a}$$

where

$$s = \sqrt{\frac{\gamma}{2}}\, M_r \tag{9b}$$

and where the relative Mach number is defined as

$$M_r = \frac{\left|\left(\vec{V}_g - \vec{V}_p\right)\right|}{\sqrt{\gamma RT}} \tag{9c}$$

For incompressible flows where $N_{Re,r} > 1$, there is a significant amount of experimental data. Empirical equations have been derived which predict these data for limited ranges of $N_{Re,r}$. The empirical C_D equation given by Torobin and Gauvin (ref. 13) is

$$C_D = \frac{24}{N_{Re,r}}\left(1 + 0.15N_{Re,r}^{0.687}\right) \tag{10}$$

Equation (10) gives good predictions of the incompressible steady-state sphere C_D data tabulated by Perry (ref. 14) for $N_{Re,r} < 200$.

For many LV applications in high-speed flows, the dependence of the drag coefficient on M_r (compressibility effect) as well as $N_{Re,r} > 1$ must be accounted for. The available C_D equations that are applicable to high-speed flow are the ones used by Cuddihy et al. (refs. 4 and 5), Carlson and Hoglund (ref. 6), Crowe (ref. 7), Crowe et al. (ref. 8), Waldman (ref. 9), and Korkan et al. (ref. 10). These equations are longer and more detailed than equations (8) to (10) given above, and are given in the appendix.

To date LV researchers have used several different C_D equations for particle-motion calculations. Asher et al. (ref. 15), assuming small velocity lags, use Stokes drag equation (8) to determine turbulence velocity spectra. In their early work at Mach 3, Yanta et al. (ref. 16) used the following incompressible C_D equation from reference 17:

$$C_D = 28N_{Re,r}^{-0.85} + 0.48 \tag{11}$$

In later work at the same Mach number, Yanta (refs. 18 and 19) uses the C_D equation from references 4 and 5. In an LV application study at Mach 5, Meyers and Walsh (ref. 2) also use the method from references 4 and 5. Maxwell and Seasholtz (ref. 11) examined particle motion through a normal shock for a free-stream Mach number 1.6, and Maxwell (ref. 20) computed particle motion through turbomachinery using the C_D of Carlson and

Hoglund. Morse et al. (ref. 21) examined particle motion in a Mach 5 flow using an earlier version of Crowe's method.

In considering the various C_D equations that have been used in past LV studies, it is important to determine which equation is the most applicable to LV studies. The next sections examine the available experimental sphere C_D data and compare the predictions of the C_D equations in references 4 to 10 to the sphere C_D data to determine the most suitable equation for LV use.

Experimental Data

A review of the literature which studies drag coefficient of spheres indicates that Bailey and Hiatt (ref. 22) provide the most extensive sphere C_D data available. The $M_r < 2$ and $N_{Re,r} < 200$ range covered by the experimental C_D data of Bailey and Hiatt (ref. 22) and of references 23 to 27 are shown in figure 1. Figure 1 indicates that the Bailey and Hiatt data cover a significant part of the $N_{Re,r} < 200$ range and the $M_r < 2$ range that was not covered by previous data. Figure 2 shows that the variation of the previous drag coefficient data of references 23 to 29 and the Bailey and Hiatt data is less than 2 percent in the $N_{Re,r}$ range 10^5 to 10^6 and as much as 13 percent at the lower $N_{Re,r}$ $(N_{Re,r} = 30, \quad M_r = 2)$.

Bailey (ref. 30) has examined some experimental factors, such as turbulence and model support interference, that affect the sphere C_D measurements; his study has shown that most of the early sphere drag data are in reasonable agreement with the Bailey and Hiatt data if these factors are accounted for. Zarin has observed that turbulence has little effect on C_D for $N_{Re,r} < 100$ if the turbulence intensities are below 3 percent. Aroesty (ref. 31) and Sherman (ref. 32) have also noted that model support interference may cause large errors in C_D measurements. The only data shown in figures 1 and 2 that are free of model support interference and turbulence effects are the data of Bailey and Hiatt, of Zarin, and of Goin and Lawrence. The data of Goin and Lawrence are limited but show excellent agreement with the data of Bailey and Hiatt. As shown in figure 1, the data of Zarin cover a lower M_r range than the data of Bailey and Hiatt. Therefore, the combined data of Zarin and of Bailey and Hiatt provide the most complete and accurate coverage of the M_r and $N_{Re,r}$ range encountered in partical-motion studies connected with LV systems. The following section compares the C_D equations of references 4 to 10 to this sphere C_D data.

Selection of the Most Applicable C_D for LV Studies

The equations of references 9 and 10 are the only ones of references 4 to 10 that were published after the Bailey and Hiatt sphere C_D data became available. Without referencing any new data, Waldman (ref. 9) modified the earlier method of Crowe (ref. 7);

Korkan, Petrie, and Bodonyi (ref. 10) used the data of Bailey and Hiatt (ref. 22). A comparison of the equations used in references 4 and 5 with the equations in reference 10 (see appendix), together with a comparison of the parameter values in tables I and II, indicate that there is little difference between the two methods except for the temperature correction used in reference 10 and differences in the continuum C_D values $C_{D,C}$. The value of $C_{D,C}$ is the value of C_D at large $N_{Re,r}$. Therefore, the method used in reference 10 has only modified the high $N_{Re,r}$ predictions of references 4 and 5.

Figure 3 compares the predictions of the six C_D equations of references 4 to 10 with experimental sphere C_D data to determine the best C_D equation available. For the comparisons in figure 3, the particle or sphere temperature is assumed to be equal to the gas temperature (the condition of the experimental data). As noted earlier, reference 10 used only the higher $N_{Re,r}$ data of reference 22. Figure 3 shows that the method of Korkan et al. fails to predict the data of reference 22 for $N_{Re,r} < 100$. Figure 3 also shows that the other methods (refs. 4 to 9) do not give good predictions of low $N_{Re,r}$ and M_r sphere C_D data.

Better Predictions for C_D

In this section the method used by Cuddihy, Beckwith, and Schroeder (refs. 4 and 5) is modified to give better predictions of the experimental sphere C_D data of references 22 and 26. For $M_r \geq 0.5$, the method given in references 4 and 5 used the following equation:

$$C_D = C_{D,C} + \left(C_{D,FM} - C_{D,C}\right) \exp\left[-A\left(N_{Re,r}\right)^N\right] \tag{12}$$

where $C_{D,C}$ and $C_{D,FM}$ are the continuum and the free-molecular values of C_D, respectively. The parameters A and N are functions of M_r and are selected to fit experimental sphere C_D data. With suitable mathematical operations, equation (12) becomes

$$\log_e\left[\log_e\left(C_{D,FM} - C_{D,C}\right) - \log_e\left(C_D - C_{D,C}\right)\right] = \log_e A + N \log_e N_{Re,r} \tag{13}$$

which is the equation of a straight line in the coordinates

$$\left[\log_e\left(\log_e \frac{C_{D,FM} - C_{D,C}}{C_D - C_{D,C}}\right); \log_e N_{Re,r}\right]$$

A least squares fit of available experimental sphere C_D data then yields the value of A and N.

This paper uses equation (12) for $M_r \geq 0.1$ and adjusts the parameters A and N to fit the experimental C_D data of references 22 and 26. Also, the C_D values are required to approach the incompressible C_D values of equation (10) as M_r approaches 0.1 and compressibility becomes negligible. The new values for the parameters $C_{D,C}$, C_D, A, and N in equation (12) are given in table III. The values for $C_{D,C}$ are obtained from the high $N_{Re,r}$ data of reference 22. These values were selected on the basis that $C_{D,C}$ is the value C_D approaches at large $N_{Re,r}$. Thus, $C_{D,C}$ can be tabulated as a function of M_r. For LV applications, the gas molecules would reflect from the particles diffusively; therefore, the $C_{D,FM}$ values are determined by use of equation (9) which assumes diffuse reflection. The values of $C_{D,FM}$ used by references 4 and 5 for their particle-motion studies were the values of $C_{D,FM}$, assuming specular reflection.

Figure 4 indicates that the method presented here gives excellent predictions of the experimental C_D data. These equations do not account for differences between particle temperature and gas temperature since there is no reliable experimental data on which to base a temperature correction for relative Mach numbers less than 2.

The small region of extrapolation in this approach ($M_r < 1.0$; $N_{Re,r} < 40$) can be further reduced by introducing into the experimental data base any new low relative Mach number and Reynolds number data that become available. Based on comparisons, it has been found that equation (12), with the parameter values given in table III, gives the best predictions of sphere C_D data; therefore, it is more applicable to particle-motion studies in connection with LV systems. The next section examines the influence of C_D on particle motion for a limited number of high-speed gas flows.

Effect of C_D on Particle-Motion Calculations

As mentioned earlier, particle motion is sensitive to the size, mass density, and initial velocity of the particle as well as to the gas flow-field properties. This report is concerned only with the influence of C_D on the particle-motion calculations. This influence is determined by examining a limited number of high-speed flows that may be encountered in LV applications.

Table IV lists the stagnation pressure, stagnation temperature, gas velocities, maximum M_r and $N_{Re,r}$ encountered by the particles during the calculation, and the location in the flow where the particle-velocity calculations are compared. Table V lists the dimensions of the nozzles that are important to the particle-motion calculations. The particle-mass density for all the test cases was equal to 919.5 kg/m^3. It should be noted that the location of comparison is arbitrary and that the particle velocity lag varies with

distance. Thus, the differences between the particle velocities predicted using the various C_D equations may increase or decrease with a change in the comparison location. For all the test cases where the particles traversed a shock, the initial particle velocity was assumed to be equal to the free-stream gas velocity ahead of the shock. For the Mach 5 and Mach 6 center-line test cases, the particles were injected upstream of the nozzle throat at a velocity equal to the gas velocity at that point, 30.48 m/s. For the Mach 3 test case, the particles were injected at the throat of the nozzle at the sonic gas velocity. As shown in tables IV and V, the comparison locations for the particles flowing along the center line of the nozzle were selected so as to be on or downstream of the nozzle exit. For the test cases involving particles traversing a shock (see figs. 5 to 7), a comparison location was arbitrarily chosen to be 1.27 cm behind the shock. For the oblique shock, the two-dimensional particle motion was calculated, whereas one-dimensional particle motion was calculated for the normal shock and the center-line nozzle test cases.

Figures 5 to 7 indicate the percent velocity lag calculated by using various C_D equations, where the percent velocity lag of the x-component is defined as

$$\theta_x \equiv \text{Percent velocity lag of x-component} = 100 \frac{V_{g,x} - V_{p,x}}{V_{g,x}} \tag{14a}$$

and that of the y-component as,

$$\theta_y \equiv \text{Percent velocity lag of y-component} = 100 \frac{V_{g,y} - V_{p,y}}{V_{g,y}} \tag{14b}$$

Figures 5 and 6 examine the influence of C_D on particle-motion calculations using both the methods from references 4 to 10 that consider compressibility and the present method; figure 7 examines the incompressible C_D equations (8) and (10) in comparison to equations used in the present method. For LV applications in high-speed flows, it is expected that particle sizes would be in the 0.5- to 2-μm range. Figures 5 to 7 show that even in this particle-size range, the percent velocity lag predicted by the previous C_D equations may vary considerably for certain flows. For example, a 0.5-μm particle passing through a normal shock in a Mach 3 flow has a particle velocity lag somewhere between 0 and 80 percent, 1.27 cm behind the shock, depending on the C_D method used. This large uncertainty in the velocity lag is caused by variations in the C_D predictions. The present method gives better predictions of the C_D sphere drag data and, therefore, better predictions of the particle motion. Figures 5 to 7 indicate the importance of using an accurate C_D equation in the regions behind normal shocks and in the y-component of particle-velocity calculations for 5^o and 10^o oblique shocks in the Mach 3 to Mach 6 flows

for the stagnation conditions listed in table IV. As mentioned earlier, the flow fields examined in this paper are limited in number and were selected only to determine whether the C_D equation used could have an important influence on particle-motion calculations. It must be noted that there may be other flow-field conditions or measuring locations where inaccurate C_D methods may lead to larger errors in particle-motion predictions than determined in this report.

Figures 5 to 7 show that large percent velocity lags occur when particles pass through a normal shock. The previous discussion has been limited to examining particle-velocity predictions behind normal shocks at 1.27 cm behind the shock. In supersonic flows where normal shocks may occur, it is important to determine how close to the shock accurate LV measurements can be made. Stokes C_D equation is often used in particle-motion calculations since it has an analytical solution for constant velocity fields. (See ref. 17.) Figures 8 to 11 present the percent velocity lag as a function of distance for the Mach 1.6 to Mach 6 normal shocks and stagnation conditions examined earlier. The calculations were performed by use of the present method and Stokes C_D equation. The figures show that the differences in velocity-lag predictions do vary with the comparison location as mentioned earlier.

Often, the distance behind the shock where particle velocity lag has decreased to a specified percent is needed. This distance is defined as the relaxation length (in cm). The specified percent used in this paper is 1 percent. Figure 12 gives the relaxation lengths for the Mach 1.6 to Mach 6 normal shocks and stagnation conditions examined previously. There are considerable differences in the calculated relaxation lengths as the particle size increases. The Stokes method predicts greater relaxation lengths than the present one for Mach 1.6 and Mach 5 (except for $D_p < 3.5$ μm) normal shocks; however, the situation is reversed for the Mach 3 and Mach 6 normal shocks. This reversal in the trends of λ with D_p is caused by the local density which is dependent on the stagnation temperature and pressure and the free-stream Mach number.

The effect of stagnation pressure on the calculation of relaxation length behind a Mach 6 normal shock is shown in figure 13. At low stagnation pressures, Stokes C_D equation predicts smaller relaxation lengths than the method used here. As the stagnation pressure increases, the present method predicts smaller relaxation lengths; however, the Stokes calculations are not affected by changes in stagnation pressure. If Stokes C_D equation (8) is substituted into equation (4), the following equation is obtained for the particle motion behind a normal shock:

$$\frac{dV_{p,x}}{dt} = \frac{18\mu_g(V_{g,x} - V_{p,x})}{\rho_p D_p^2} \tag{15}$$

Equation (15) clarifies the results shown in figures 12 and 13. Particle-motion calculations using Stokes C_D equation are independent of changes in the gas density or pressure and are affected by temperature changes only through the gas viscosity μ_g. Reference 33 indicated that stagnation temperature and free-stream Mach number have a much smaller effect than stagnation pressure on the errors in using Stokes C_D equation for particle-motion calculations. In summary, Stokes equation may be a good simple C_D equation for low stagnation pressure calculations, but it may lead to large errors at large stagnation pressures.

CONCLUDING REMARKS

A number of particle drag coefficient C_D equations are available in the literature on sphere drag coefficients. Particle motion in a number of supersonic flows was examined using these C_D equations. There was little difference in the velocity predictions for center-line nozzle flows and the horizontal components of particle velocities behind the oblique shocks. However, large variations occurred in the velocity predictions for particles passing through normal shocks and in the vertical components of particle velocities behind oblique shocks.

Available sphere C_D data provided an experimental data base that was used to evaluate the predictions of the various C_D equations. It was found that none of the available methods could accurately predict the low relative Mach number and relative Reynolds number $\left(M_r \text{ and } N_{Re,r}\right)$ experimental sphere C_D data.

A modified version of the method used by Cuddihy, Beckwith, and Schroeder has been developed to give accurate predictions of the available low $N_{Re,r}$ and M_r experimental sphere C_D data. The new method was then used to demonstrate the importance of an accurate C_D equation for particle-motion calculations behind normal shocks and calculations of the y-component of particle velocity behind 5^o and 10^o oblique shocks in Mach 3 to Mach 6 flows. Finally, it was determined that errors in using Stokes C_D equation for the calculation of relaxation lengths behind normal shocks were extremely sensitive to the stagnation pressure of the free stream. These errors increased as the stagnation pressure increased.

In conclusion, an accurate C_D method is needed for particle-motion studies required in laser velocimeter diagnostics in high-speed flows since wide variations can occur in particle-velocity calculations for some supersonic flows if the C_D method used does not accurately predict the sphere C_D data.

Langley Research Center
National Aeronautics and Space Administration
Hampton, Va. 23665
January 5, 1976

APPENDIX

DETAILS OF PREVIOUS DRAG COEFFICIENT METHODS

Any evaluation of the C_D methods that account for compressibility requires an examination of the details of the various equations. This appendix discusses the details of the individual C_D methods of references 4 to 10, and similarities are noted (to explain why all existing prediction methods fail to provide accurate predictions of low M_r and $N_{Re,r}$ experimental sphere C_D data).

Method of Cuddihy, Beckwith, and Schroeder

For M_r greater than or equal to 0.5, the C_D equation used by Cuddihy, Beckwith, and Schroeder (refs. 4 and 5) is

$$C_D = C_{D,C} + \left(C_{D,FM} - C_{D,C}\right) \exp\left[-A\left(N_{Re,r}\right)^N\right] \tag{A1}$$

The values for the continuum drag coefficient $C_{D,C}$ for $M_r = 1.6$ to 9.7 are taken from the ballistics range data of May and Witt (ref. 29) and Hodges (ref. 34) for $N_{Re,r} = 10^5$ to 10^6. The free-molecular drag coefficient values $C_{D,FM}$ are taken from Emmons (ref. 12). The data used for the evaluation of the A and N parameters are taken from the experimental data of Aroesty (ref. 23), Sreekanth (ref. 24), and Ashkenas (ref. 25). The values for the parameters $C_{D,C}$, $C_{D,FM}$, A, and N are listed in table I.

For $M_r < 0.5$, the C_D equation used by Cuddihy, Beckwith, and Schroeder (refs. 4 and 5) is based on the high $N_{Re,r}$ data (10^4 to 10^5) of Charters and Thomas (ref. 28) and the incompressible steady-state C_D curve given by Rouse (ref. 35). The resulting equation is

$$C_D = \frac{\overline{C} + \dfrac{51.1M_r}{N_{Re,r}}}{1 + 0.256M_r\left(\overline{C} + \dfrac{51.1M_r}{N_{Re,r}}\right)} \tag{A2a}$$

where

$$\overline{C} = \frac{24}{N_{Re,r}} + 0.4 + 1.6 \exp\left[-\left(0.028N_{Re,r}^{0.82}\right)\right] \tag{A2b}$$

APPENDIX

It is noted that the data of Bailey and Hiatt and of Zarin was not available when this C_D equation was developed. Figure 1 indicates the large amount of extrapolation necessary to predict C_D at low values of $N_{Re,r}$ and M_r if equations (A1) and (A2) are used.

Method of Carlson and Hoglund

Carlson and Hoglund (ref. 6) approach the development of a C_D equation by modifying the Stokes C_D equation (8) for $N_{Re,r} > 1$ as done in reference 13:

$$C_{D,inc} = \frac{24}{N_{Re,r}}\left(1 + 0.15N_{Re,r}^{0.687}\right) \tag{A3}$$

Next, equation (A3) is corrected for compressibility effects based on an empirical correlation of the high $N_{Re,r}$ sphere C_D data presented by Hoerner (ref. 36):

$$C_{D,comp} = \frac{24}{N_{Re,r}}\left(1 + 0.15N_{Re,r}^{0.687}\right)\left[1 + \exp\left(-\frac{0.427}{M_r^{4.63}} - \frac{3}{N_{Re,r}^{0.88}}\right)\right] \tag{A4}$$

Finally, using the work of Millikan (ref. 37) and the experimental data of Stalder and Zurick (ref. 38), Carlson and Hoglund modify equation (A4) to account for rarefied flow effects:

$$C_D = \frac{24}{N_{Re,r}}\left\{\frac{\left(1 + 0.15N_{Re,r}^{0.687}\right)\left[1 + \exp\left(\frac{0.427}{M_r^{4.63}} - \frac{3}{N_{Re,r}^{0.88}}\right)\right]}{1 + \frac{M_r}{N_{Re,r}}\left[3.82 + 1.28\exp\left(-1.25\frac{N_{Re,r}}{M_r}\right)\right]}\right\} \tag{A5}$$

One disadvantage of equation (A5) is that the constants 3.82 and 1.28 are evaluated to give the correct rarefied flow C_D for $M_r = 0.5$. For any other M_r, equation (A5) does not give the correct free-molecular limit of C_D.

Carlson and Hoglund could only compare the predictions of equation (A5) with Mach 2 experimental data since the lower M_r and $N_{Re,r}$ data of Bailey and Hiatt and of Zarin were not available in 1964.

Method of Crowe

A later paper by Crowe (ref. 7) compared the predictions of the equation of Carlson and Hoglund with Mach 3 experimental data and found poor agreement. Crowe then devel-

oped a C_D method that predicts Mach 3 experimental data. The equation was formulated by Crowe to give the correct value of the C_D at $M_r = 0$ and $M_r = 2$. The resulting equation is

$$C_D = (C_{D,inc} - 2) \exp \left\{-3.632\left[\frac{M_r}{N_{Re,r}} g(N_{Re,r})\right]\right\} + \frac{h(M_r)}{1.183M_r} \exp\left(-\frac{N_{Re,r}}{2M_r}\right) + 2 \qquad \text{(A6a)}$$

where

$$\log_{10} g(N_{Re,r}) = 1.25\left[1 + \tanh\left(0.77 \log_{10} N_{Re,r} - 1.92\right)\right] \qquad \text{(A6b)}$$

$$h(M_r) = 2.3 - 1.7\left(\frac{T_p}{T_g}\right)^{1/2} - 2.3 \tanh\left(1.17 \log_{10} M_r\right) \qquad \text{(A6c)}$$

Both the methods of Crowe and of Carlson and Hoglund approach the incompressible C_D values and account for compressibility effects by correlating the compressible high $N_{Re,r}$ data of Hoerner.

Method of Crowe, Babcock, and Willoughby

In a later paper Crowe, Babcock, and Willoughby (ref. 8), noting that equation (A6) exhibited an unlikely inflection point, developed a new C_D equation that depended more on experimental sphere C_D data. The basic equation of Crowe, Babcock, and Willoughby is

$$C_D = C_{D,C} + (C_{D,FM} - C_{D,C})\overline{C}_D \qquad \text{(A7)}$$

A comparison of equations (A1) and (A7) shows that

$$\overline{C}_D = \exp\left[-A(N_{Re,r})^N\right] \qquad \text{(A8)}$$

The main difference between the two equations is that the method used by Cuddihy, Beckwith, and Schroeder tabulated the parameters $C_{D,C}$, $C_{D,FM}$, A, and N as given in table I, and Crowe, Babcock, and Willoughby provided equations for the various parameters $C_{D,C}$, $C_{D,FM}$, and $\overline{C}_D$. Also, Crowe, Babcock, and Willoughby were able to base their equation on additional experimental sphere C_D data that had become available since the development of the method used by Cuddihy, Beckwith, and Schroeder. The $C_{D,FM}$

values for equation (A7) were obtained from equation (9) given by Emmons, and the $C_{D,C}$ data were taken from an empirical correlation of the compressible C_D data of Hoerner as given below

$$C_{D,C} = 0.66 + 0.26 \tanh \left(2 \log_e M_r\right) + 0.17 \exp \left[-2.5\left(\frac{\log_e M_r}{1.4}\right)^2\right] \tag{A9}$$

A comparison of equations (A5), (A6), and (A9), makes it difficult to see any similarities even though Hoerner's data were used for the correlations in all three equations. The equation for $\overline{C}_D$ in equation (A7) was determined by correlating the experimental data of Aroesty (ref. 23), May and Witt (ref. 29), Sims (ref. 39), Sivier and Nicholls (ref. 40) Zarin (ref. 26), and Millikan (ref. 37) among others. The resulting equation for $\overline{C}_D$ is

$$\overline{C}_D = \frac{K}{K+1}\left\{1 - \exp\left[-BN_{Kn}^{0.6} \exp\left(N_{Kn}\right)\right]\right\} \tag{A10a}$$

where

$$K = N_{Kn}^{0.4} \exp\left(1.2\sqrt{N_{Kn}}\right) \tag{A10b}$$

$$B = \frac{\left(C_{D,inc} - 0.4\right)N_{Re,r}}{8} \tag{A10c}$$

Method of Waldman

Waldman (ref. 9) modified Crowe's method to account for the transonic drag rise at high Reynolds number without making any reference to additional data. The resulting equation used by Waldman is

$$C_D = \left[C_{D,inc} - 2 + 0.463F(M_r)\right] \exp\left[-\frac{M_r}{N_{Re,r}} z\left(N_{Re,r}\right)\right] + R(M_r) \exp\left(-0.5\frac{N_{Re,r}}{M_r}\right) + 2 \tag{A11a}$$

where

$$F(M_r) = \exp\left(\frac{0.863}{M_r{}^2} - \frac{1.163}{M_r{}^4}\right) \tag{A11b}$$

$$z(N_{Re,r}) = 3.632 \exp\left(\frac{4}{46.5N_{Re,r}^{-0.667} + 1}\right) \tag{A11c}$$

$$R(M_r) = \frac{1}{1.183M_r}\left[\frac{4.65}{M_r + 1} + 1.67\left(\frac{T_p}{T_g}\right)^{1/2}\right] \tag{A11d}$$

Method of Korkan, Petrie, and Bodonyi

The latest method found in the literature is the method of Korkan, Petrie, and Bodonyi (ref. 10) who compared the drag coefficient equations of Cuddihy, Beckwith, and Schroeder, of Carlson and Hoglund, and of Crowe to the 1971 sphere drag data of Bailey and Hiatt. They determined that the method used by Cuddihy, Beckwith, and Schroeder gives the best prediction of the Bailey and Hiatt data. The equations as presented in reference 10 are slightly different from the equations used by Cuddihy, Beckwith, and Schroeder. Private communication with the author of reference 10 confirmed that for $M_r < 0.5$ the drag coefficient equation should be identical to equation (A2) originally used by Cuddihy, Beckwith, and Schroeder. Also, for $M_r \geq 0.5$ the drag coefficient equation should be identical to equation (A1) used by Cuddihy, Beckwith, and Schroeder except for the addition of a temperature correction term, $\Delta C_D(T)$, and the $C_{D,C}$ parameters in equation (A1). The new $C_{D,C}$ values are listed in table II. Equation (A1) used in reference 10 with a temperature correction term is given below:

$$C_D = C_{D,C} + \left(C_{C,FM} - C_{D,C}\right) \exp\left[-A\left(N_{Re,r}\right)^N\right] + \Delta C_D(T) \tag{A12a}$$

where for $M_r > 1$

$$\Delta C_D(T) = \frac{\frac{T_p}{T_g} - 1}{1.183M_r}\left[0.142 + \left(2.22 - 0.597\sqrt{\frac{T_p}{T_g}}\right) \exp\left(\frac{-N_{Re,r}}{M_r}\right)\right] \tag{A12b}$$

and for $M_r < 1$

$$\Delta C_D(T) = 0 \tag{A12c}$$

In summary, the only improvement of the method of reference 10 over the one used in references 4 and 5 would be the predicted C_D values for high values of $N_{Re,r}$.

REFERENCES

1. Mie, G.: Optics of Turbid Media. Ann. Phys., vol. 25, no. 3, 1908, pp. 377-445.

2. Meyers, James F.; and Walsh, Michael J.: Computer Simulation of a Fringe Type Laser Velocimeter. Paper presented at Workshop on Laser Velocimetry (Purdue Univ., West Lafayette, Indiana), Mar. 1974.

3. Soo, S. L.: Fluid Dynamics of Multiphase Systems. Blaisdell Publ. Co., c.1967.

4. Cuddihy, W. F.; Beckwith, I. E.; and Schroeder, L. C.: A Solution to the Problem of Communications Blackout of Hypersonic Reentry Vehicles. Paper presented at Anti-Missile Research Advisory Council Meeting (Annapolis, Md.), Oct. 1963.

5. Cuddihy, William F.; Beckwith, Ivan E.; and Schroeder, Lyle C. (appendix A by Ivan E. Beckwith, Dennis M. Bushnell, and James L. Hunt; appendix B by Ivan E. Beckwith and Sadie P. Livingston; and appendix C by Ivan E. Beckwith): Flight Test and Analysis of a Method for Reducing Radio Attenuation During Hypersonic Flight. NASA TM X-1331, 1967.

6. Carlson, Donald J.; and Hoglund, Richard F.: Particle Drag and Heat Transfer in Rocket Nozzles. AIAA J., vol. 2, no. 11, Nov. 1964, pp. 1980-1984.

7. Crowe, C. T.: Drag Coefficient of Particles in a Rocket Nozzle. AIAA J., vol. 5, no. 5, May 1967, pp. 1021-1022.

8. Crowe, C. T.; Babcock, W. R.; and Willoughby, P. G.: Drag Coefficient for Particles in Rarefied, Low-Mach Number Flows. International Symposium on Two-Phase Systems (Haifa, Israel), Aug.-Sept. 1971.

9. Waldman, George D.: Parametric Study for a Conceptual Multicomponent Flow System. ARL 74-0030, AVCO Systems Div., May 1974. (Available from DDC as AD-783 213.)

10. Korkan, K. D.; Petrie, S. L.; and Bodonyi, R. J.: Particle Concentrations in High Mach Number Two-Phase Flows. AIAA Paper No. 74-606, July 1974.

11. Maxwell, Barry R.; and Seasholtz, Richard G.: Velocity Lag of Solid Particles in Oscillating Gases and in Gases Passing Through Normal Shock Waves. NASA TN D-7490, 1974.

12. Emmons, Howard W., ed.: Fundamentals of Gas Dynamics. Vol. III. Princeton Univ. Press, 1958.

13. Torobin, L. B.; and Gauvin, W. H.: Fundamental Aspects of Solids-Gas Flow. Can. J. Chem. Eng., vol. 37, no. 4, Aug. 1959, pp. 129-141.

14. Perry, John H., ed.: Chemical Engineers' Handbook. Third ed., McGraw-Hill Book Co., Inc., 1950.

15. Asher, J. A.; Scott, P. F.; and Wang, J. C.: Parameters Affecting Laser Velocimeter Turbulence Spectra Measurements. AEDC-TR-74-54, U.S. Air Force, Oct. 1974. (Available from DDC as AD-786 886/2GA.)

16. Yanta, W. J.; Gates, D. F.; and Brown, F. W.: The Use of a Laser Doppler Velocimeter in Supersonic Flow. AIAA Paper No. 71-287, Mar. 1971.

17. Gilbert, Mitchell; Davis, Leo; and Altman, David: Velocity Lag of Particles in Linearly Accelerated Combustion Gases. Jet Propulsion, vol. 25, no. 1, Jan. 1955, pp. 26-30.

18. Yanta, William J.: Measurements of Aerosol Size Distributions With a Laser Doppler Velocimeter (LDV). AIAA Paper No. 73-705, July 1973.

19. Yanta, William J.: Turbulence Measurements With a Laser Doppler Velocimeter. NOL-TR-73-94, Naval Air Systems Command, May 1973. (Available from DDC as AD-766 781.)

20. Maxwell, Barry E.: Particle Flow in Blade Passage of Turbomachinery With Application to Laser-Doppler Velocimetry. NASA CR-134543, 1974.

21. Morse, Howard L.; Tullis, Barclay J.; Seifert, Howard S.; and Babcock, Wayne: Development of a Laser-Doppler Particle Sensor for the Measurement of Velocities in Rocket Exhausts. J. Spacecraft & Rockets, vol. 6, no. 3, Mar. 1969, pp. 264-272.

22. Bailey, A. B.; and Hiatt, J.: Free-Flight Measurements of Sphere Drag at Subsonic, Transonic, Supersonic, and Hypersonic Speeds for Continuum, Transition, and Near-Free-Molecular Flow Conditions. AEDC-TR-70-291, U.S. Air Force, Mar. 1971. (Available from DDC as AD 721 208.)

23. Aroesty, Jerome: Sphere Drag in a Low Density Supersonic Flow. Rep. No. HE-150-192 (Contract N-onr-222(45)), Inst. Eng. Res., Univ. of California, Jan. 3, 1962.

24. Sreekanth, A. K.: Drag Measurements on Circular Cylinders and Spheres in the Transition Regime at a Mach Number of 2. Rep. No. 74, Inst. Aerophys., Univ. of Toronto, Apr. 1961.

25. Ashkenas, Harry: Low-Density Sphere Drag With Equilibrium and Nonequilibrium Wall Temperature. Rarefied Gas Dynamics, Vol. II, J. A. Laurmann, ed., Academic Press, 1963, pp. 278-290.

26. Zarin, Neil A.: Measurement of Non-Continuum and Turbulence Effects on Subsonic Sphere Drag. NASA CR-1585, 1970.

27. Goin, Kennith L.; and Lawrence, W. R.: Subsonic Drag of Spheres at Reynolds Numbers From 200 to 10,000. AIAA J. (Tech. Notes), vol. 6, no. 5, May 1968, pp. 961-962.

28. Charters, Alex C.; and Thomas, Richard N.: The Aerodynamic Performance of Small Spheres From Subsonic to High Supersonic Velocities. Rep. No. 514, Ballistic Res. Labs., Aberdeen Proving Ground, May 1, 1945.

29. May, Albert; and Witt, W. R., Jr.: Free-Flight Determinations of the Drag Coefficients of Spheres. J. Aeron. Sci., vol. 20, no. 9, Sept. 1953, pp. 635-638.

30. Bailey, A. B.: Sphere Drag Coefficient for Subsonic Speeds in Continuum and Free-Molecule Flows. J. Fluid Mech., vol. 65, pt. 2, Aug. 28, 1974, pp. 401-410.

31. Aroesty, Jerome: Sphere Drag in a Low-Density Supersonic Flow. Rarefied Gas Dynamics, Vol. II, J. A. Laurmann, ed., Academic Press, Inc., 1963, pp. 261-277.

32. Sherman, Frederick S.: Note on Sphere Drag Data. J. Aeronaut. Sci., vol. 18, no. 8, Aug. 1951, p. 566.

33. Walsh, Michael J.: Influence of Drag Coefficient Equations on Particle Motion Calculations. Paper presented at Symposium on Laser Anemometry (Bloomington, Minnesota), Oct. 1975.

34. Hodges, A. J.: The Drag Coefficient of Very High Velocity Spheres. J. Aeronaut. Sci., vol. 24, no. 10, Oct. 1957, pp. 755-758.

35. Rouse, Hunter: Elementary Mechanics of Fluids. John Wiley & Sons, Inc., c.1946.

36. Hoerner, Sighard F.: Fluid-Dynamic Drag. Publ. by the author (148 Busteed Drive, Midland Park, New Jersey 07432), 1965.

37. Millikan, R. A.: Law of Fall of a Sphere Through a Gas and the Nature of Molecular Reflection. Phys. Rev., vol. 22, July 1923, pp. 1-23.

38. Stalder, Jackson R.; and Zurick, Vernon J.: Theoretical Aerodynamic Characteristics of Bodies in a Free-Molecule-Flow Field. NACA TN 2423, 1951.

39. Sims, William H.: Experimental Sphere Drag Results in the Near-Free Molecule Regime. Rarefied Gas Dynamics, Volume I, Leon Trilling and Harold Y. Wachman, eds., Academic Press, 1969, pp. 751-756.

40. Sivier, Kenneth R.; and Nicholls, J. A.: Subsonic Sphere Drag Measurements at Intermediate Reynolds Numbers. NASA CR-1392, 1969.

TABLE I.- PARAMETERS IN DRAG COEFFICIENT EXPRESSION

[From refs. 4 and 5]

M_r	$C_{D,C}$	$C_{D,FM}$	A	N
0.5	0.520	7.80	0.315	0.410
.6	.551	6.50	.240	.460
.7	.586	5.57	.182	.500
.8	.625	4.92	.141	.545
.9	.666	4.45	.110	.590
1.0	.712	4.10	.090	.620
1.2	.801	3.60	.065	.670
1.4	.880	3.23	.055	.690
1.6	.929	2.98	.049	.710
1.8	.955	2.80	.047	.715
2.0	.971	2.68	.046	.720

TABLE II.- PARAMETERS IN DRAG COEFFICIENT EXPRESSION

[From ref. 10]

M_r	$C_{D,C}$	$C_{D,FM}$	A	N
0.5	0.48	7.80	0.315	0.410
.6	.455	6.50	.240	.468
.7	.497	5.57	.182	.500
.8	.535	4.92	.141	.545
.9	.610	4.45	.110	.590
1.0	.820	4.10	.090	.620
1.1	.900	3.85	.070	.645
1.2	.990	3.60	.065	.670
1.3	.993	3.42	.060	.680
1.4	.995	3.23	.055	.690
1.5	.999	3.11	.052	.700
1.6	1.000	2.98	.049	.710
1.7	1.020	2.89	.048	.713
1.8	1.005	2.80	.047	.715
1.9	.990	2.74	.047	.718
2.0	1.045	2.68	.046	.720

TABLE III.- PARAMETERS IN PRESENT DRAG COEFFICIENT EXPRESSION

M_r	$C_{D,C}$	$C_{D,FM}$	A	N
0.1	0.380	53.541	1.7269	0.1976
.15	.381	35.759	1.4099	.2196
.2	.390	26.888	1.1908	.2399
.25	.392	21.580	1.0339	.2562
.3	.398	18.053	.9144	.2706
.35	.403	15.544	.8159	.2846
.4	.410	13.670	.7356	.2973
.45	.419	12.222	.6672	.3097
.5	.426	11.065	.6085	.3215
.55	.435	10.125	.5637	.3301
.6	.443	9.345	.5244	.3384
.65	.453	8.688	.4890	.3467
.7	.466	8.128	.4602	.3536
.75	.480	7.645	.4367	.3585
.8	.500	7.224	.4163	.3630
.85	.513	6.853	.4043	.3620
.9	.540	6.525	.3909	.3631
.95	.600	6.233	.4735	.3096
1.0	.710	5.970	.4384	.3086
1.1	.780	5.517	.4332	.3059
1.2	.820	5.141	.4261	.3036
1.3	.860	4.823	.4252	.3003
1.4	.890	4.551	.4260	.2969
1.5	.910	4.316	.4334	.2895
1.6	.920	4.110	.4392	.2826
1.7	.930	3.930	.4483	.2747
1.8	.940	3.771	.4535	.2696
1.9	.940	3.630	.4545	.2649
2.0	.940	3.505	.4489	.2640

TABLE IV.- GAS FLOW-FIELD PARAMETERS FOR TEST CASES FOR VELOCITY-LAG CALCULATIONS SHOWN IN FIGURES 5 TO 7

Type of flow	P_0		T_0, K	$V_{g,x}$, m/s	$V_{g,y}$, m/s	$M_{r,max}$	$N_{Re,r,max}$	Location of comparison
	10^5 N/m^2	atm						
M_∞ = 1.6, normal shock	1.013	1	283	218.4	0	0.7	118	1.27 cm behind shock
M_∞ = 3, nozzle center line	1.013	1	293	616.8	0	.8	35	7.62 cm downstream of throat
M_∞ = 3, normal shock	1.013	1	293	159.9	0	1.4	10	1.27 cm behind shock
M_∞ = 3, 5° oblique shock	1.013	1	293	596.6	52.5	.3	8	1.27 cm behind shock
M_∞ = 3, 10° oblique shock	1.013	1	293	564.1	59.4	.3	12	1.27 cm behind shock
M_∞ = 5, nozzle center line	3.446	3.4	363	783.4	0	.9	90	54.61 cm downstream of throat
M_∞ = 5, normal shock	3.446	3.4	363	156.7	0	1.7	56	1.27 cm behind shock
M_∞ = 5, 5° oblique shock	3.446	3.4	363	765.7	66.7	.4	8	1.27 cm behind shock
M_∞ = 5, 10° oblique shock	3.446	3.4	363	736.9	129.9	.7	18	1.27 cm behind shock
M_∞ = 6, nozzle center line	3.446	3.4	554	997.4	0	.8	45	168.6 cm downstream of throat
M_∞ = 6, normal shock	3.446	3.4	554	189.2	0	1.7	16	1.27 cm behind shock
M_∞ = 6, 5° oblique shock	3.446	3.4	554	977.4	85.6	.5	3	1.27 cm behind shock
M_∞ = 6, 10° oblique shock	3.446	3.4	554	945.2	166.7	.9	6	1.27 cm behind shock

TABLE V.- CENTER-LINE NOZZLE DIMENSIONS

Center-line nozzle flow	M_∞ = 3	M_∞ = 5	M_∞ = 6
Distance from upstream injection point to throat, cm	0.0	15.24	9.2
Distance from throat to nozzle exit, cm	7.62	30.48	168.6

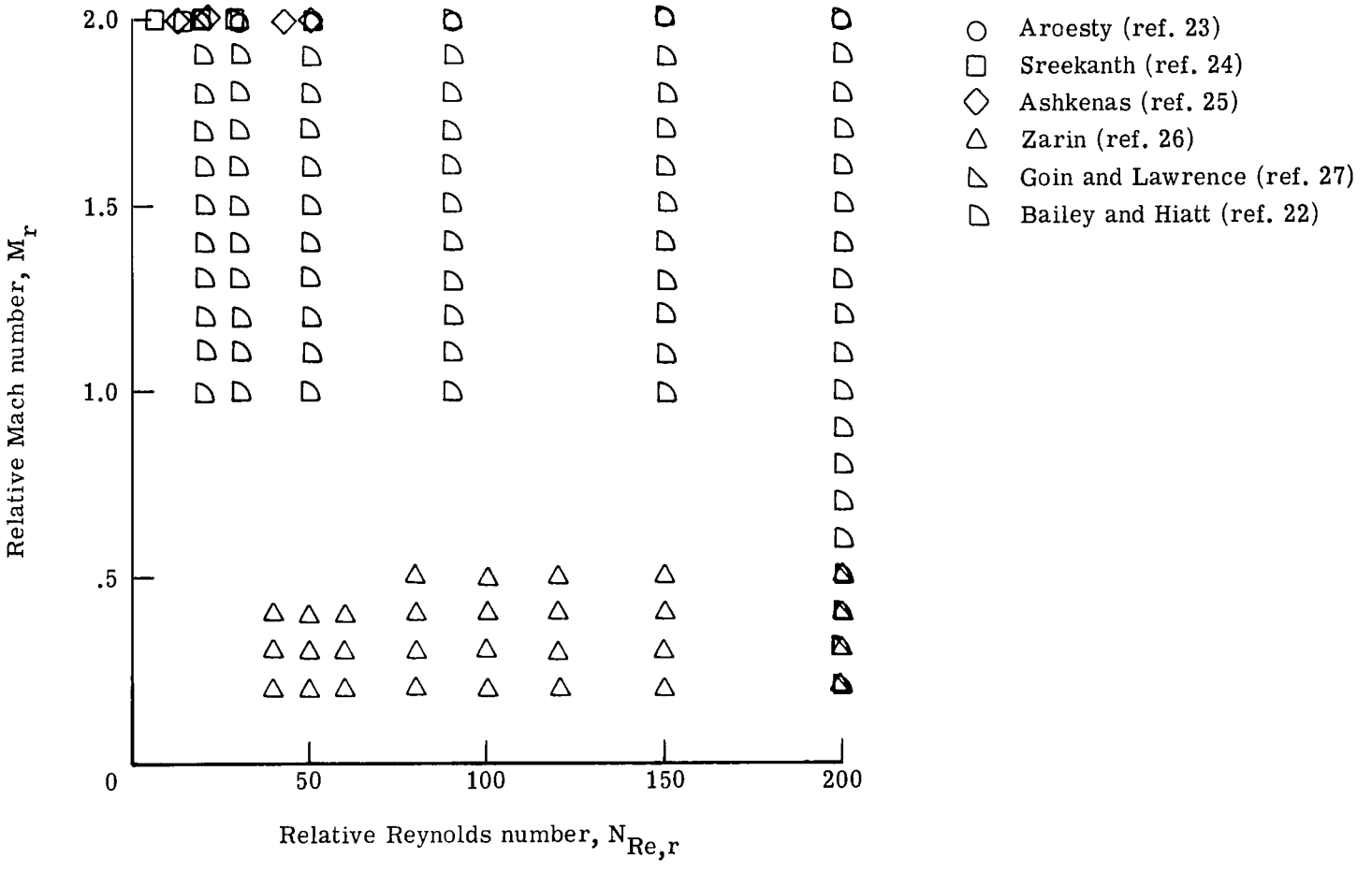

Figure 1.- Summary of available low Reynolds number and low Mach number experimental sphere drag data.

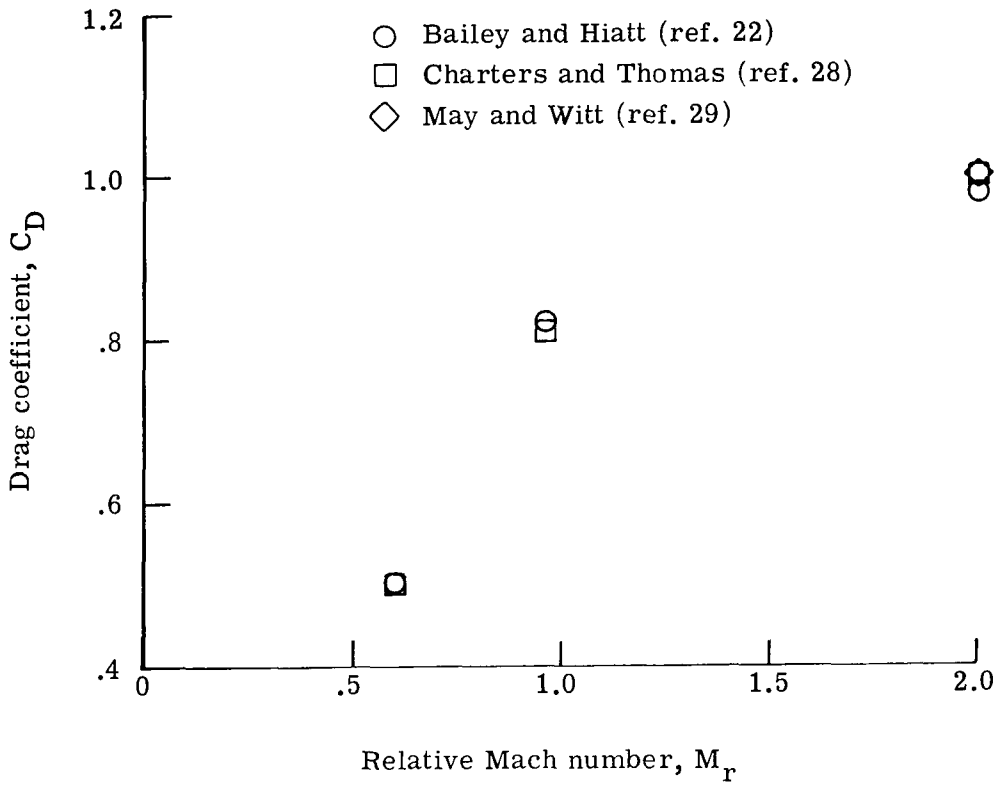

(a) High Reynolds number (10^5 to 10^6).

Figure 2.- Comparison of available experimental sphere drag data.

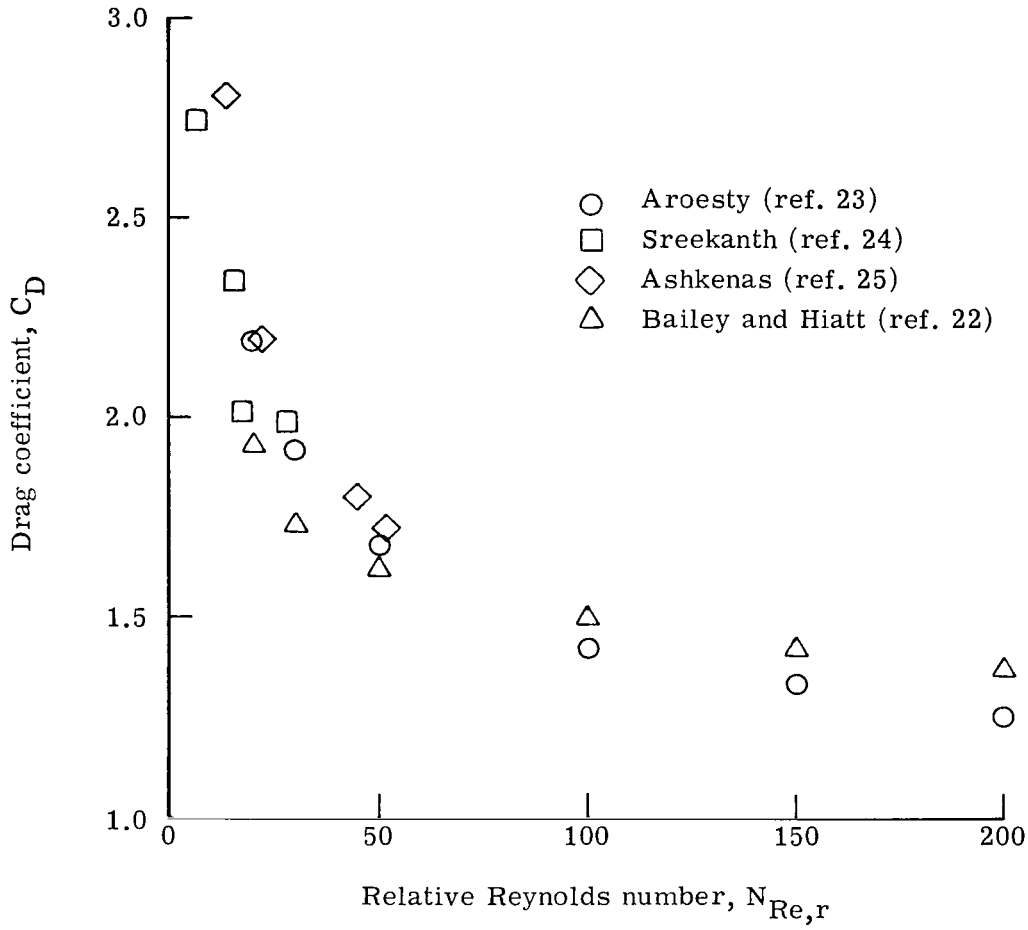

(b) $M_r = 2$.

Figure 2.- Continued.

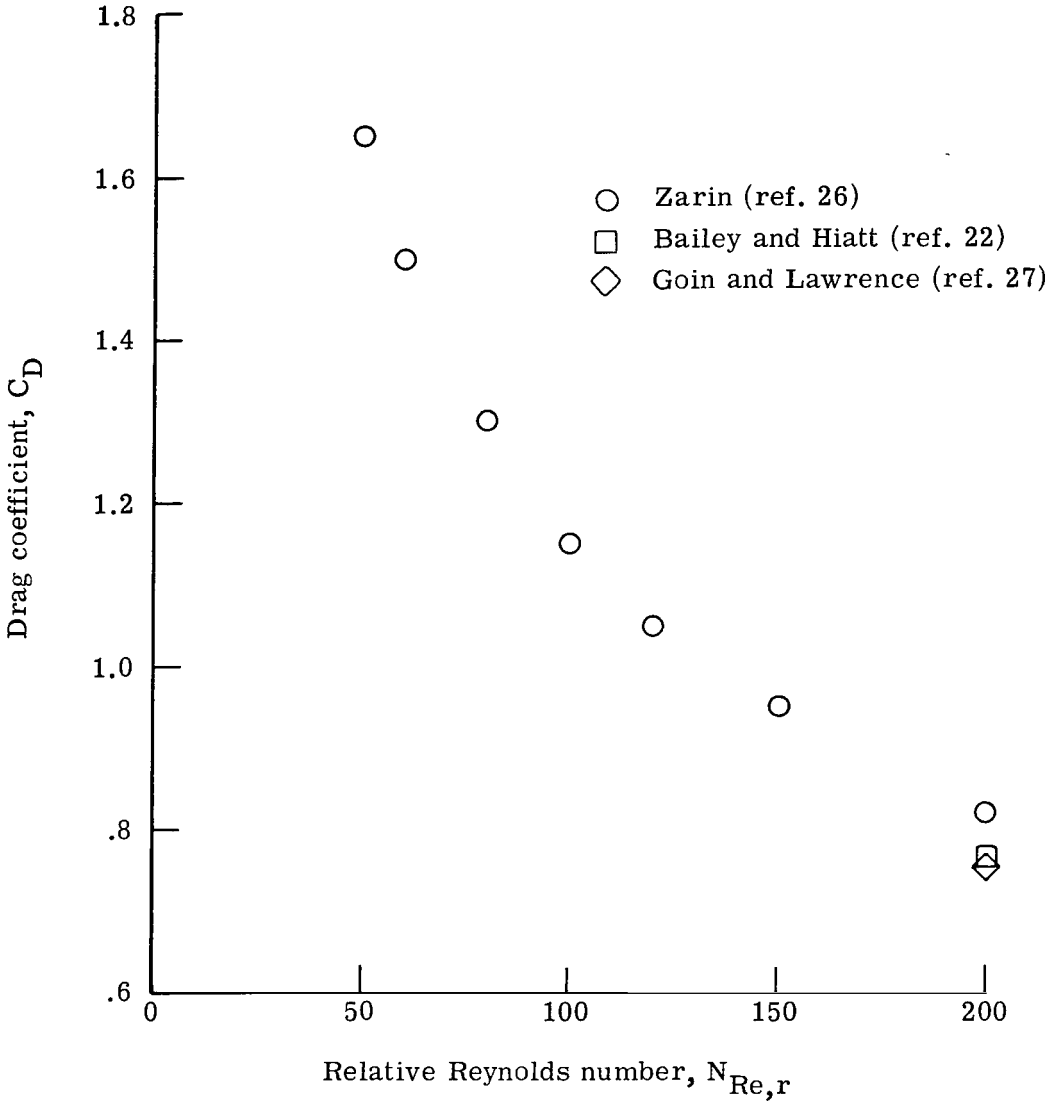

(c) $M_r = 0.2$.

Figure 2.- Concluded.

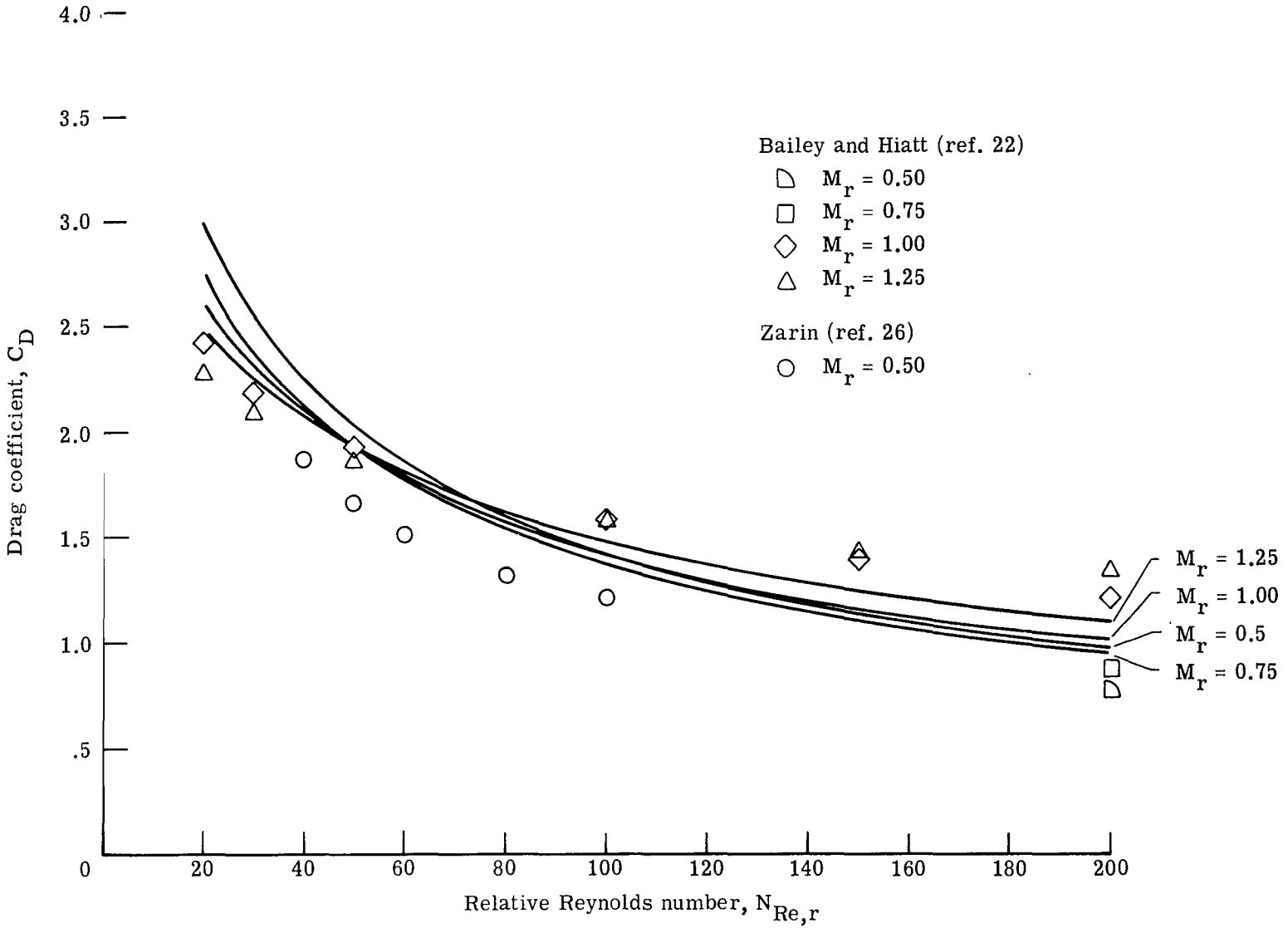

(a) Cuddihy, Beckwith, and Schroeder (refs. 4 and 5).

Figure 3.- Predictions of drag coefficient equations compared to experimental data.

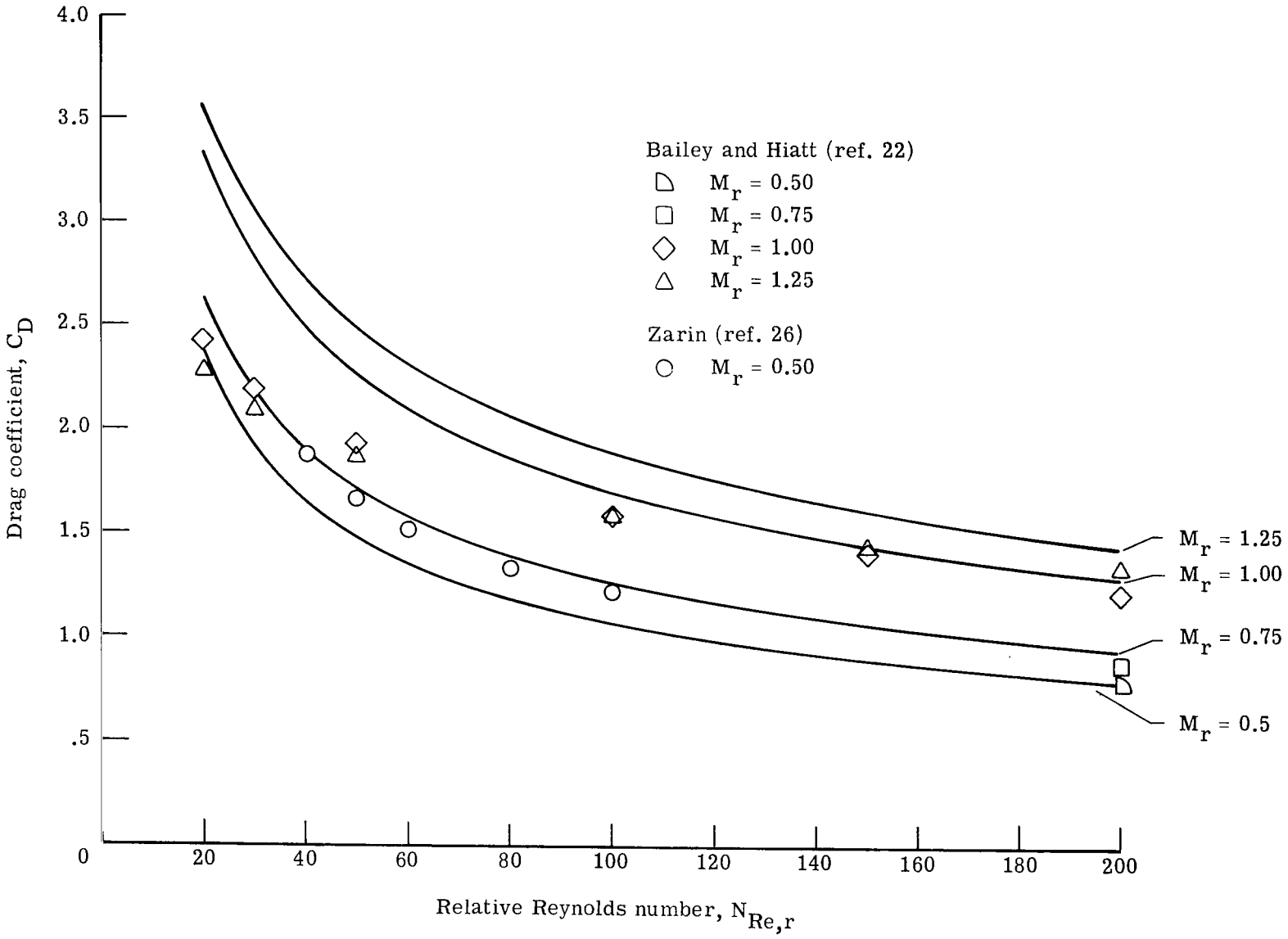

(b) Carlson and Hoglund (ref. 6).

Figure 3.- Continued.

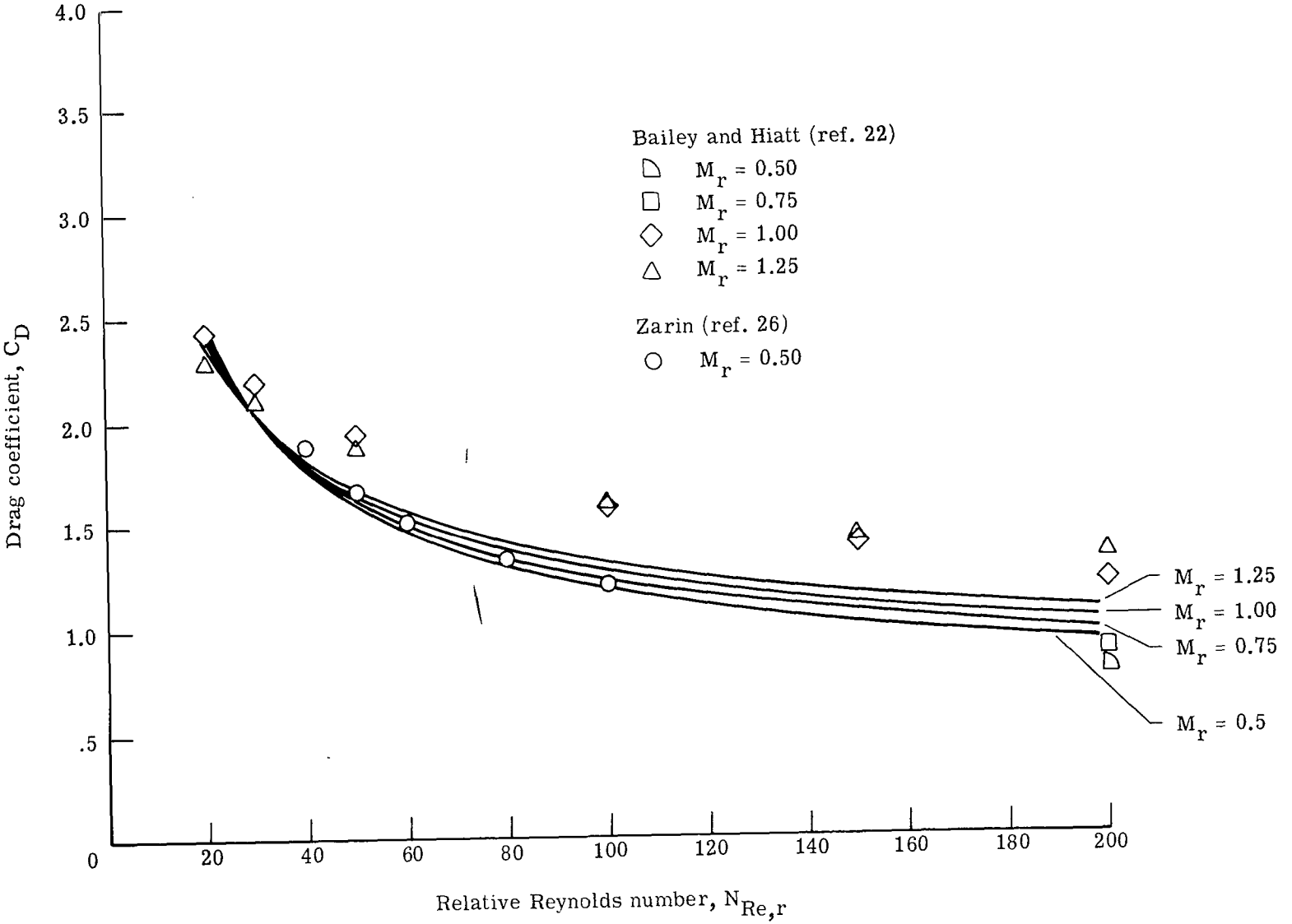

(c) Crowe (ref. 7).

Figure 3.- Continued.

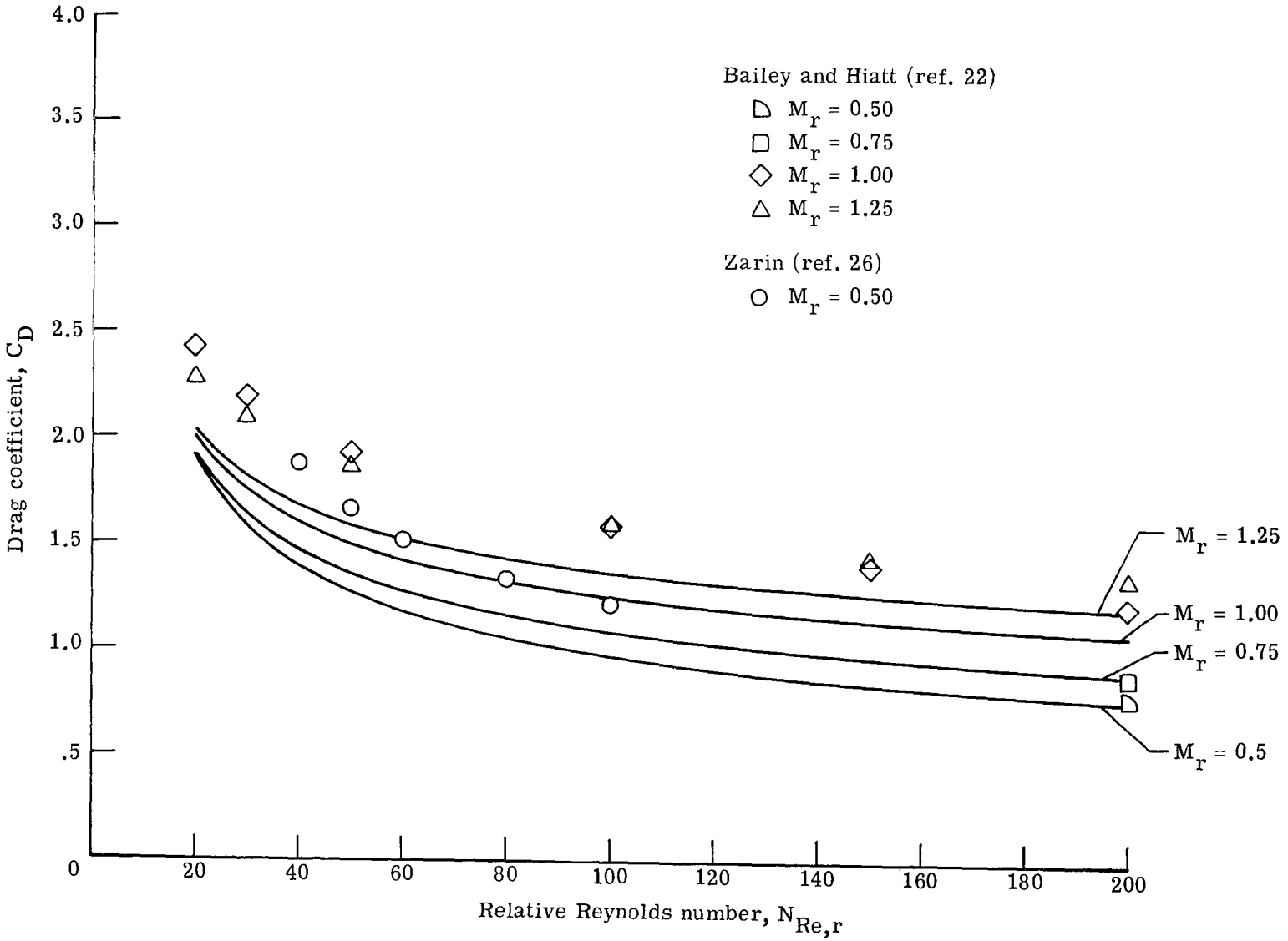

(a) Crowe, Babcock, and Willoughby (ref. 8).

Figure 3.- Continued.

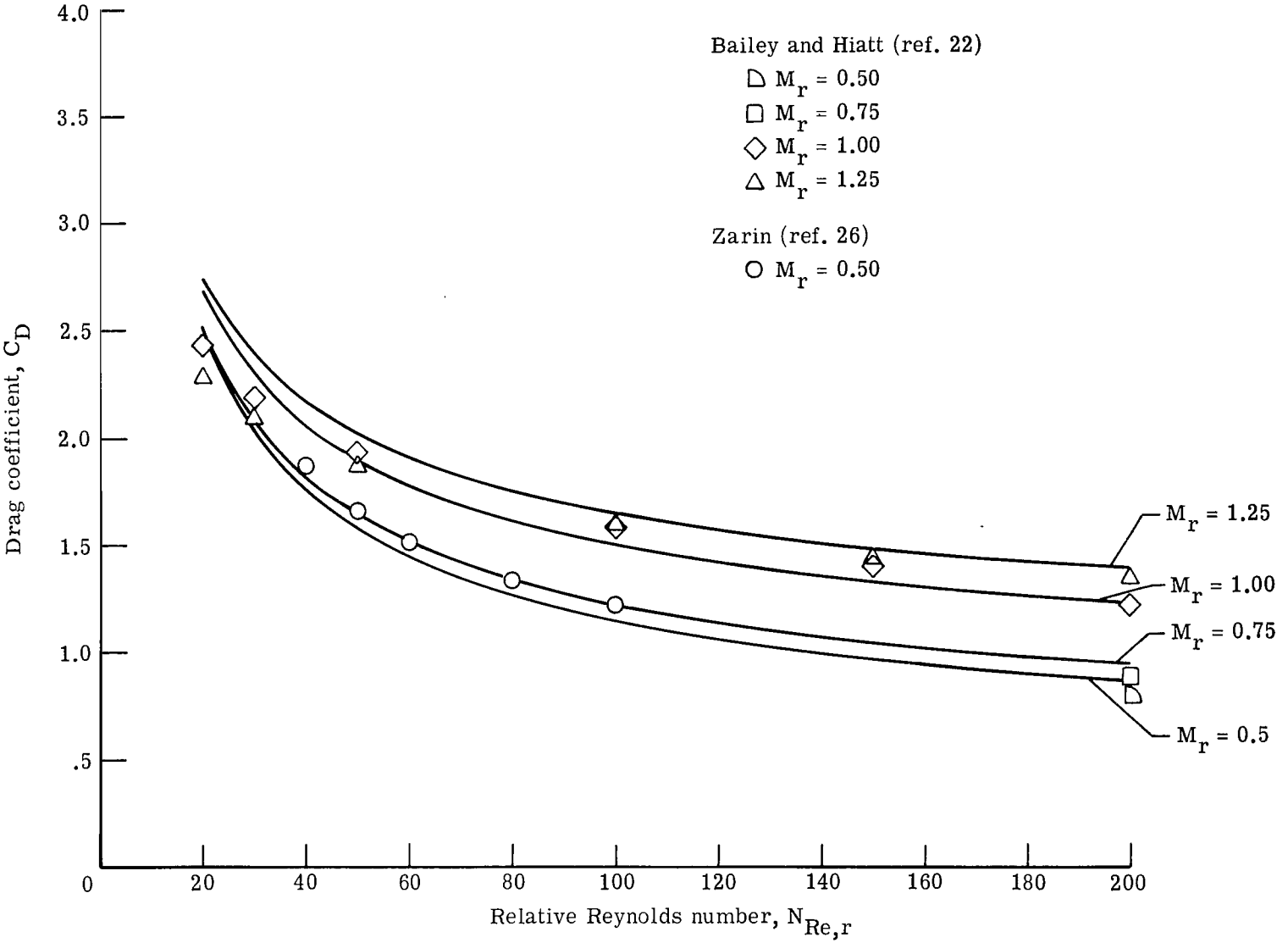

(e) Waldman (ref. 9).

Figure 3.- Continued.

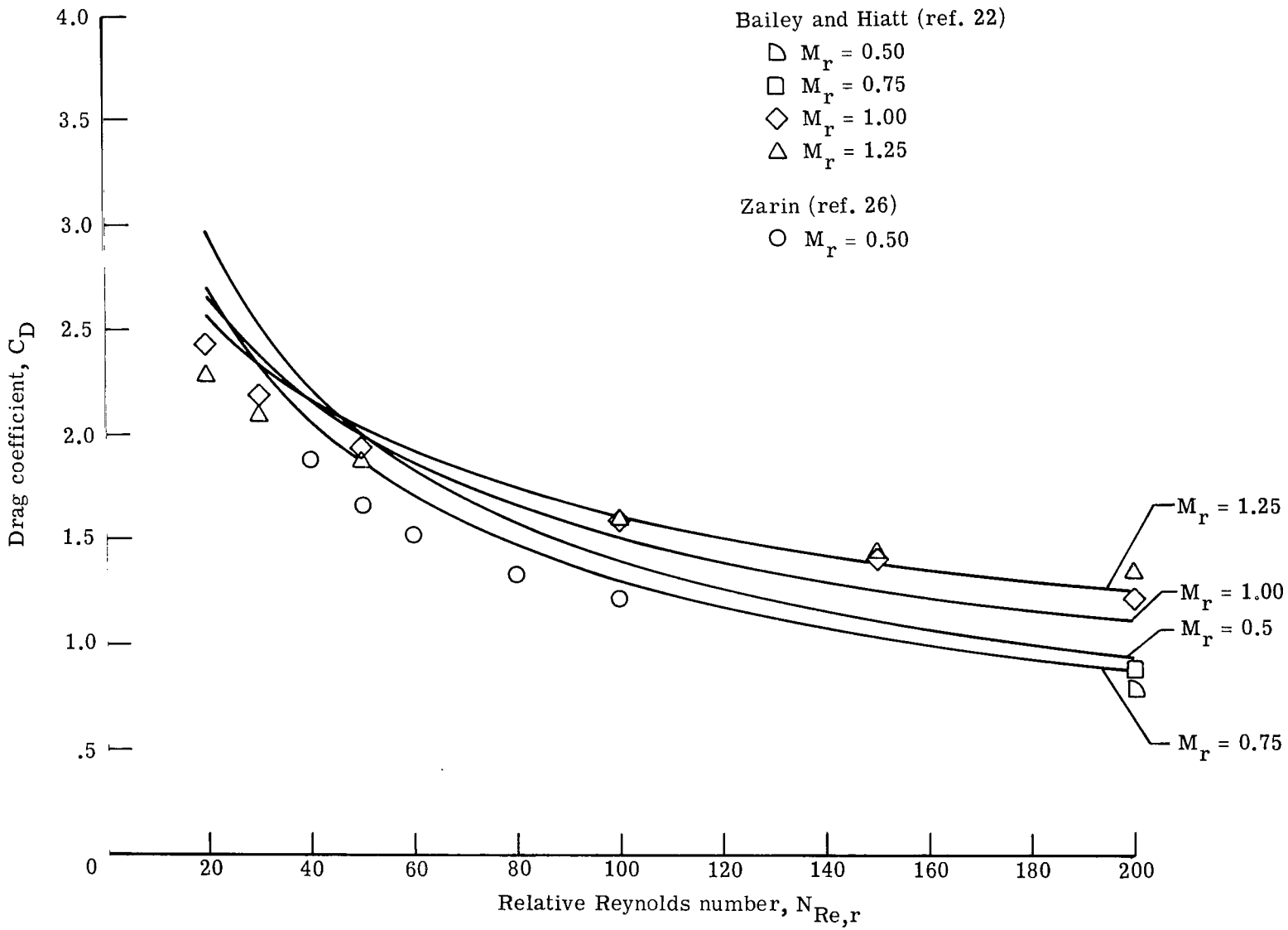

(f) Korkan, Petrie, and Bodonyi (ref. 10).

Figure 3.- Concluded.

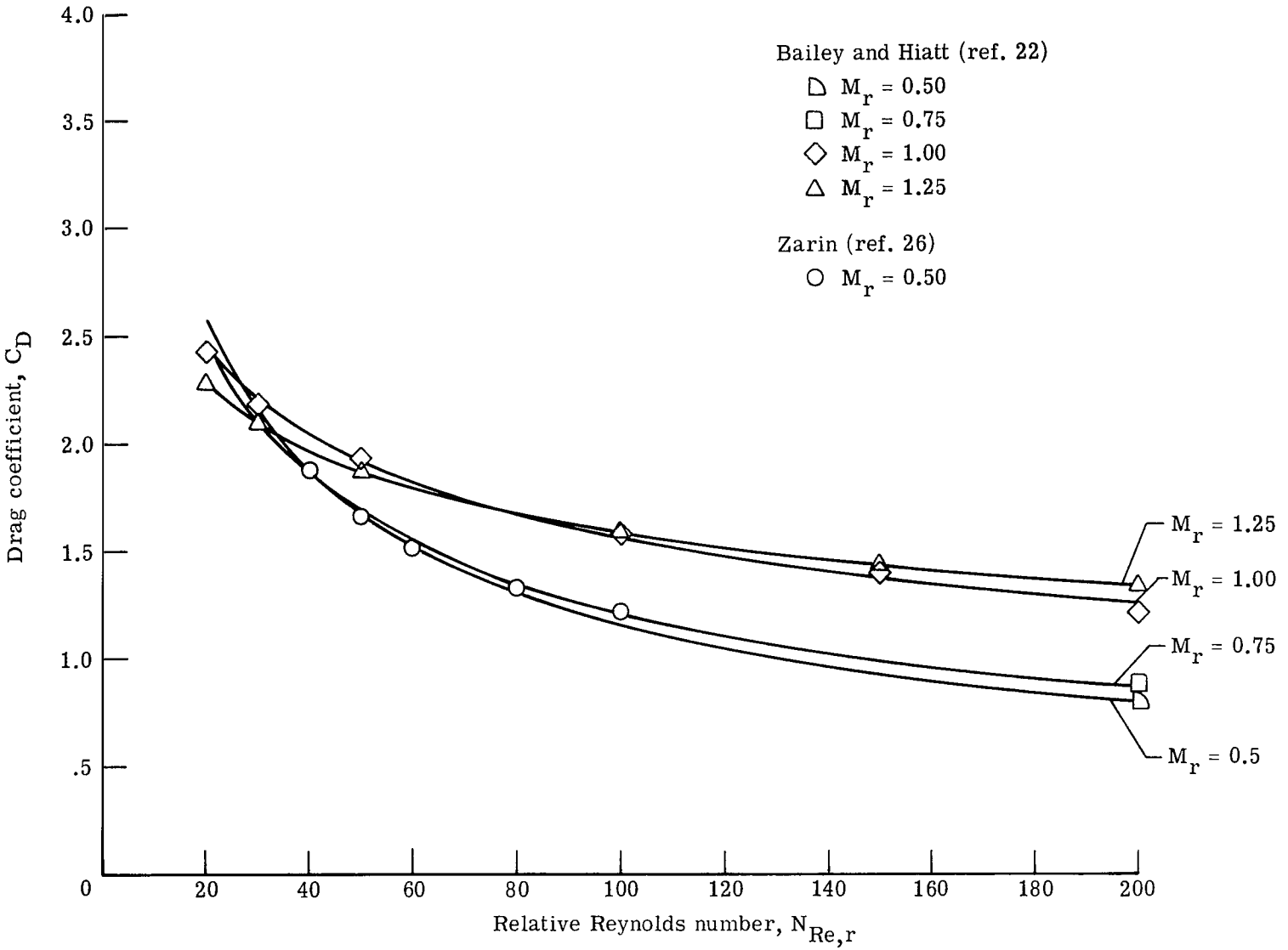

Figure 4.- Comparison of present C_D method with experimental data.

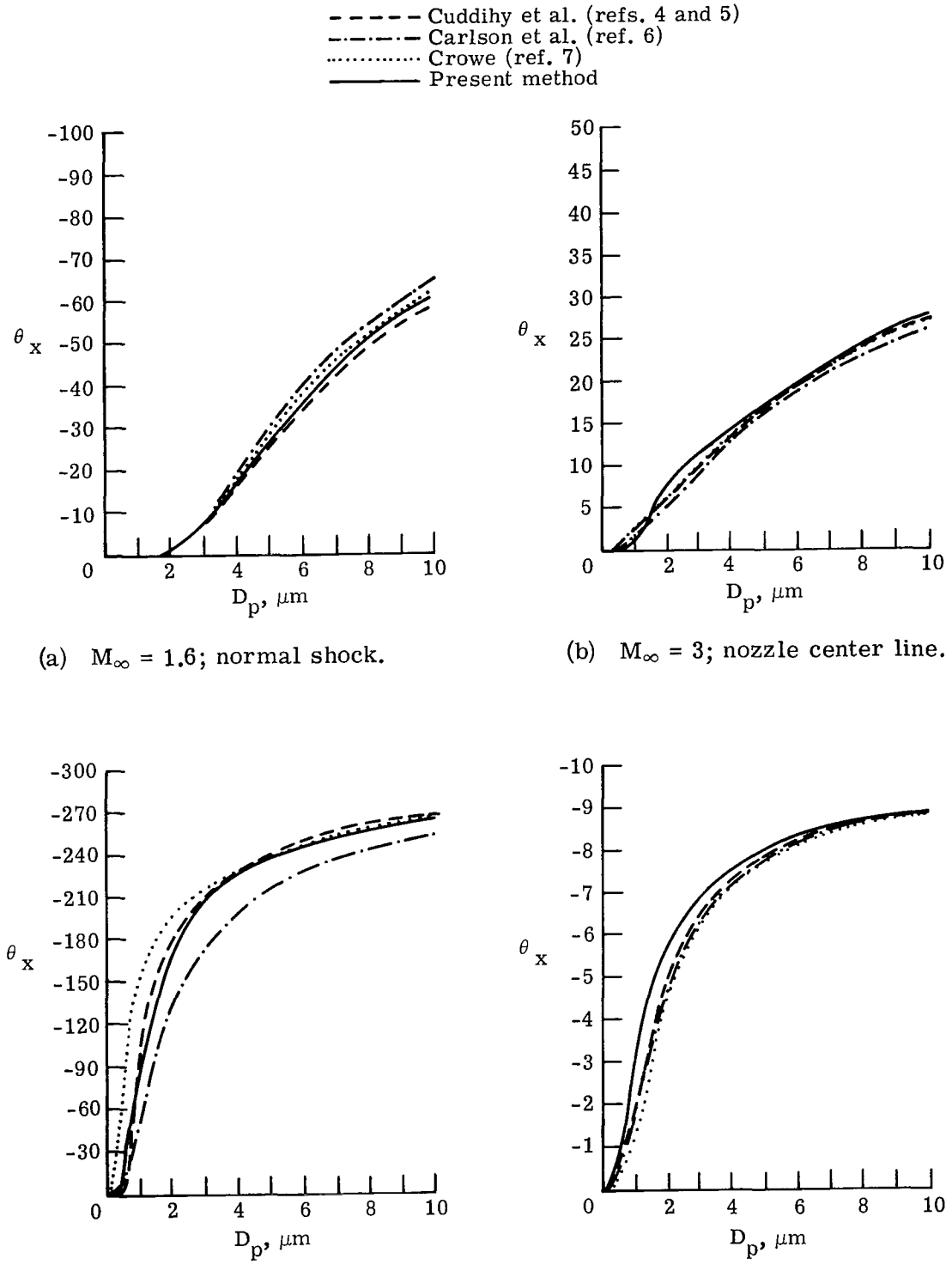

(a) $M_\infty = 1.6$; normal shock.

(b) $M_\infty = 3$; nozzle center line.

(c) $M_\infty = 3$; normal shock.

(d) $M_\infty = 3$; 10^o oblique shock x-component.

Figure 5.- At the points noted in table IV, percent velocity lag predicted by various methods.

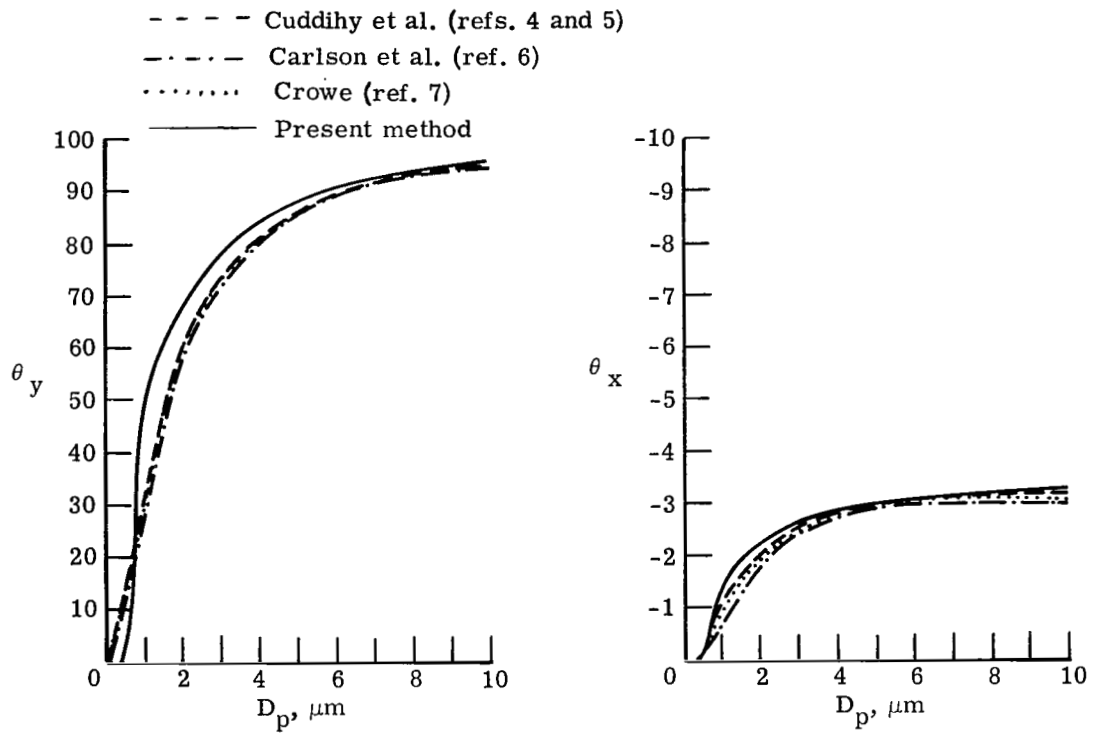

(e) $M_\infty = 3$; 10^o oblique shock y-component. (f) $M_\infty = 3$; 5^o oblique shock x-component.

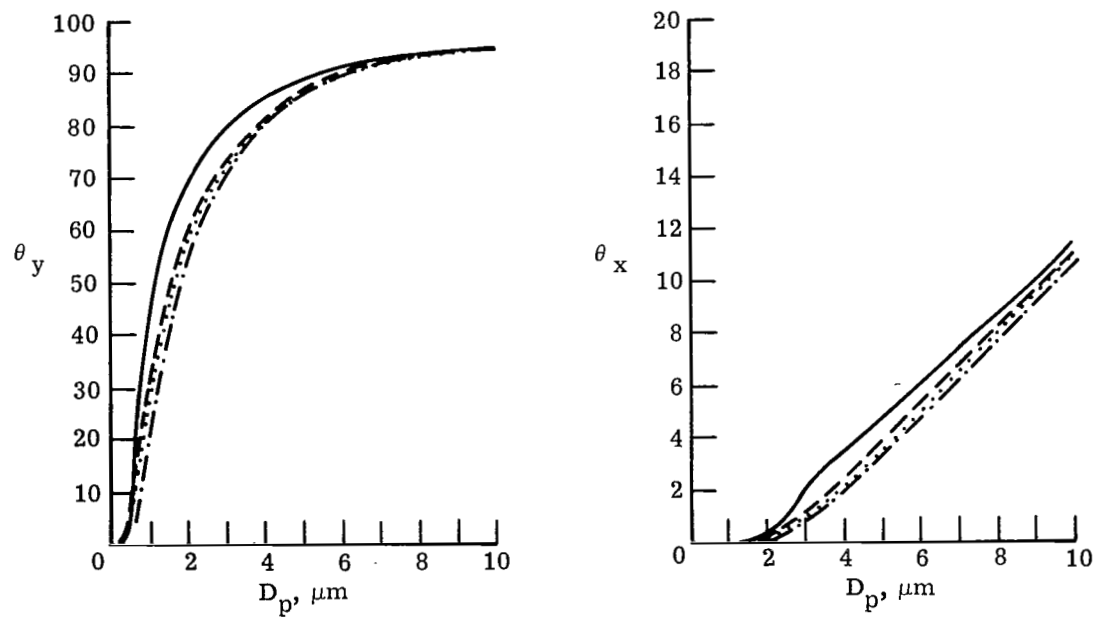

(g) $M_\infty = 3$; 5^o oblique shock y-component. (h) $M_\infty = 5$; nozzle center line.

Figure 5.- Continued.

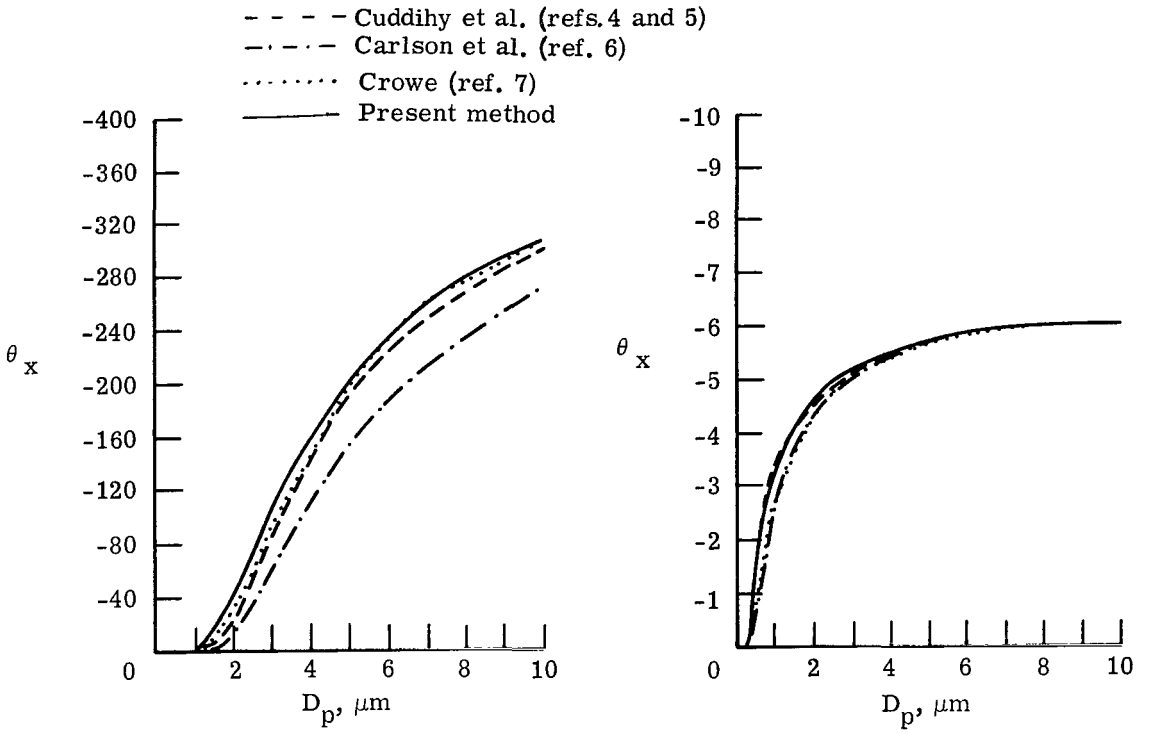

(i) $M_\infty = 5$; normal shock.

(j) $M_\infty = 5$, 10^o oblique shock x-component.

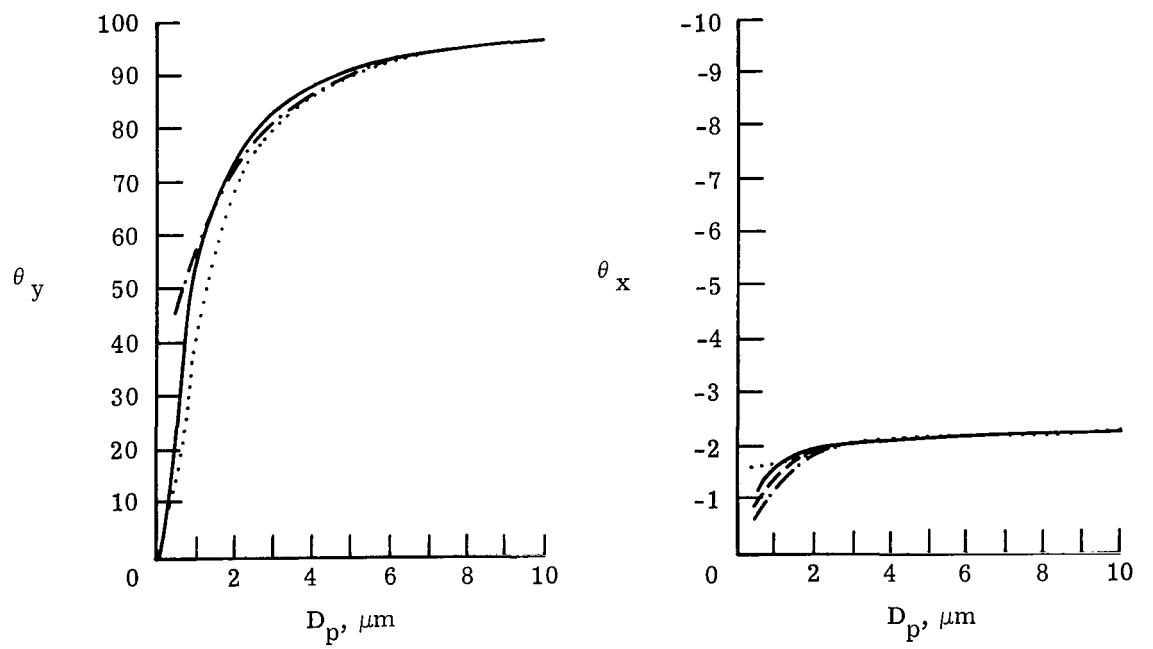

(k) $M_\infty = 5$; 10^o oblique shock y-component.

(l) $M_\infty = 5$; 5^o oblique shock x-component.

Figure 5.- Continued.

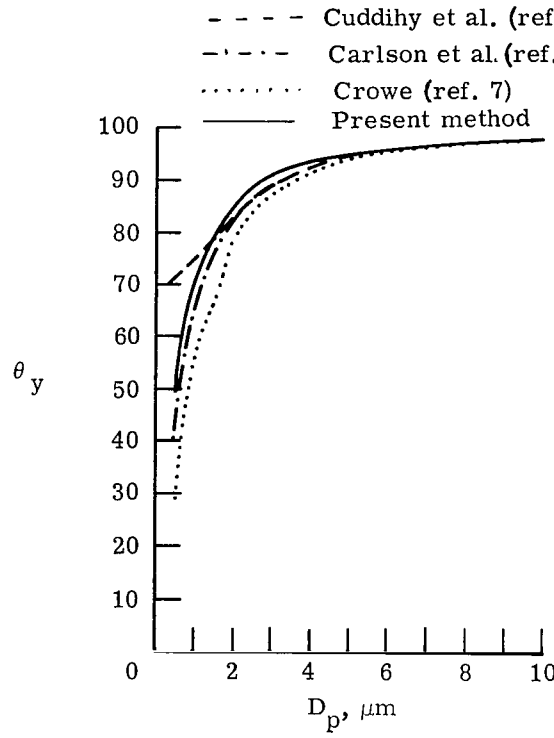

(m) $M_\infty = 5$; 5^o oblique shock y-component.

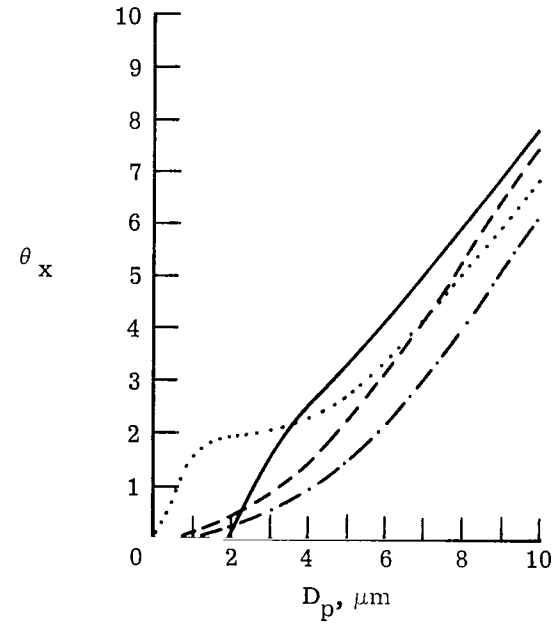

(n) $M_\infty = 6$; nozzle center line.

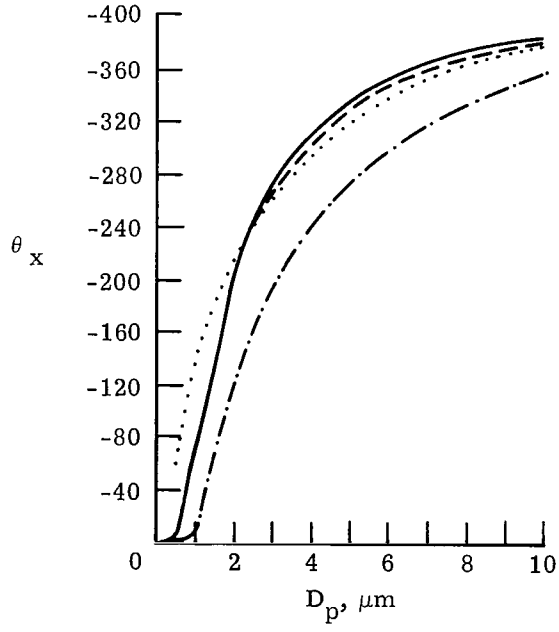

(o) $M_\infty = 6$; normal shock.

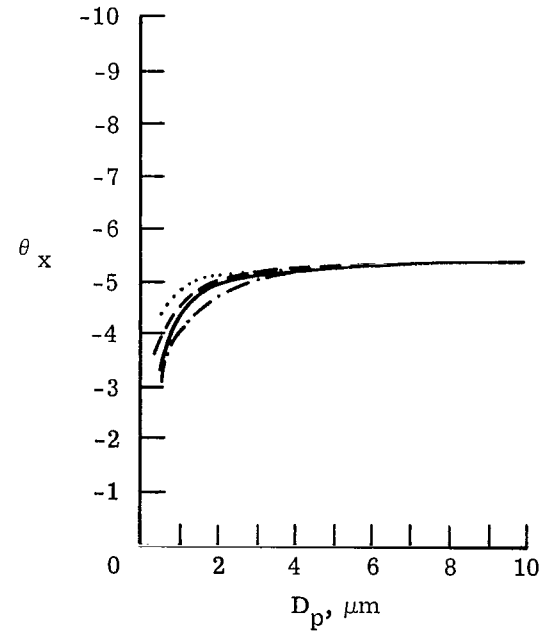

(p) $M_\infty = 6$; oblique shock x-component.

Figure 5.- Continued.

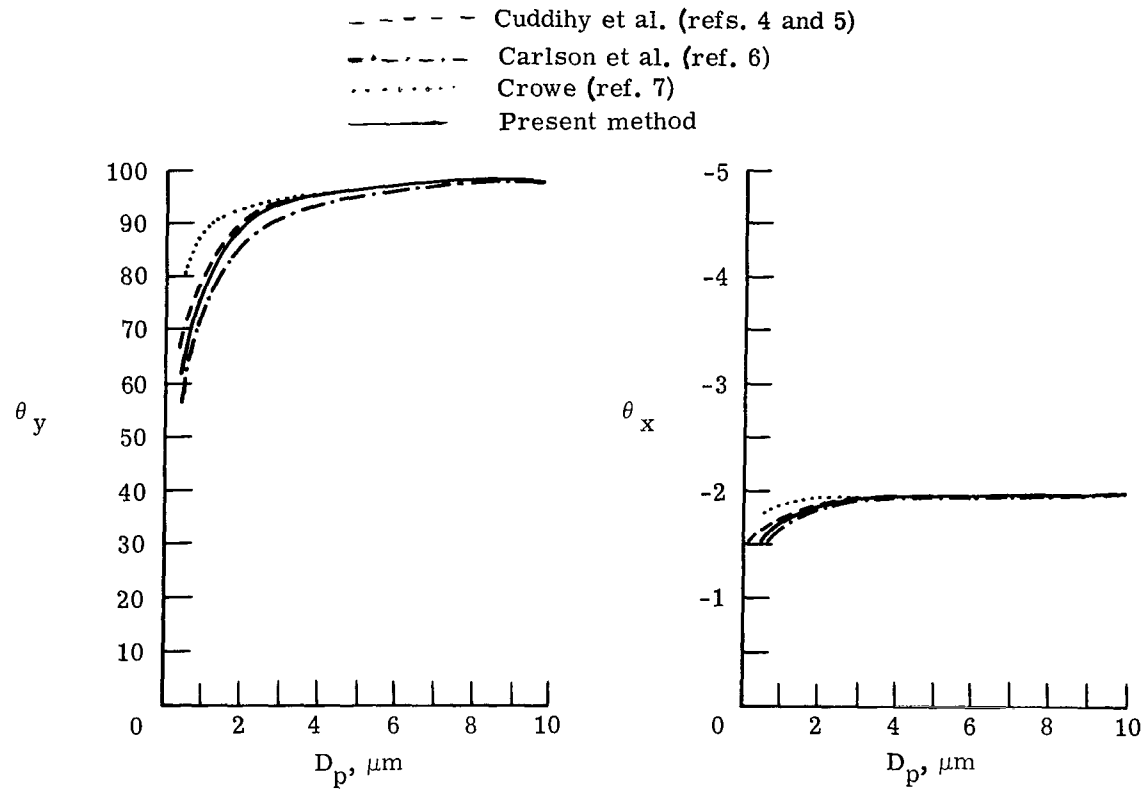

(q) $M_\infty = 6$; 10^o oblique shock y-component. (r) $M_\infty = 6$; 5^o oblique shock x-component.

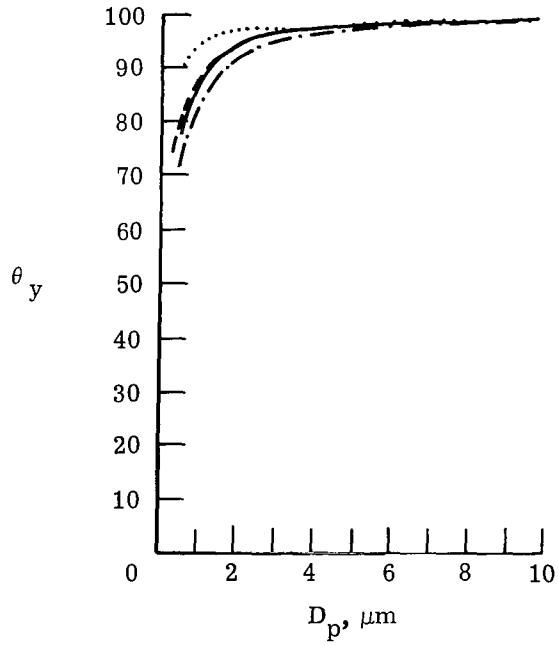

(s) $M_\infty = 6$; 5^o oblique shock x-component.

Figure 5.- Concluded.

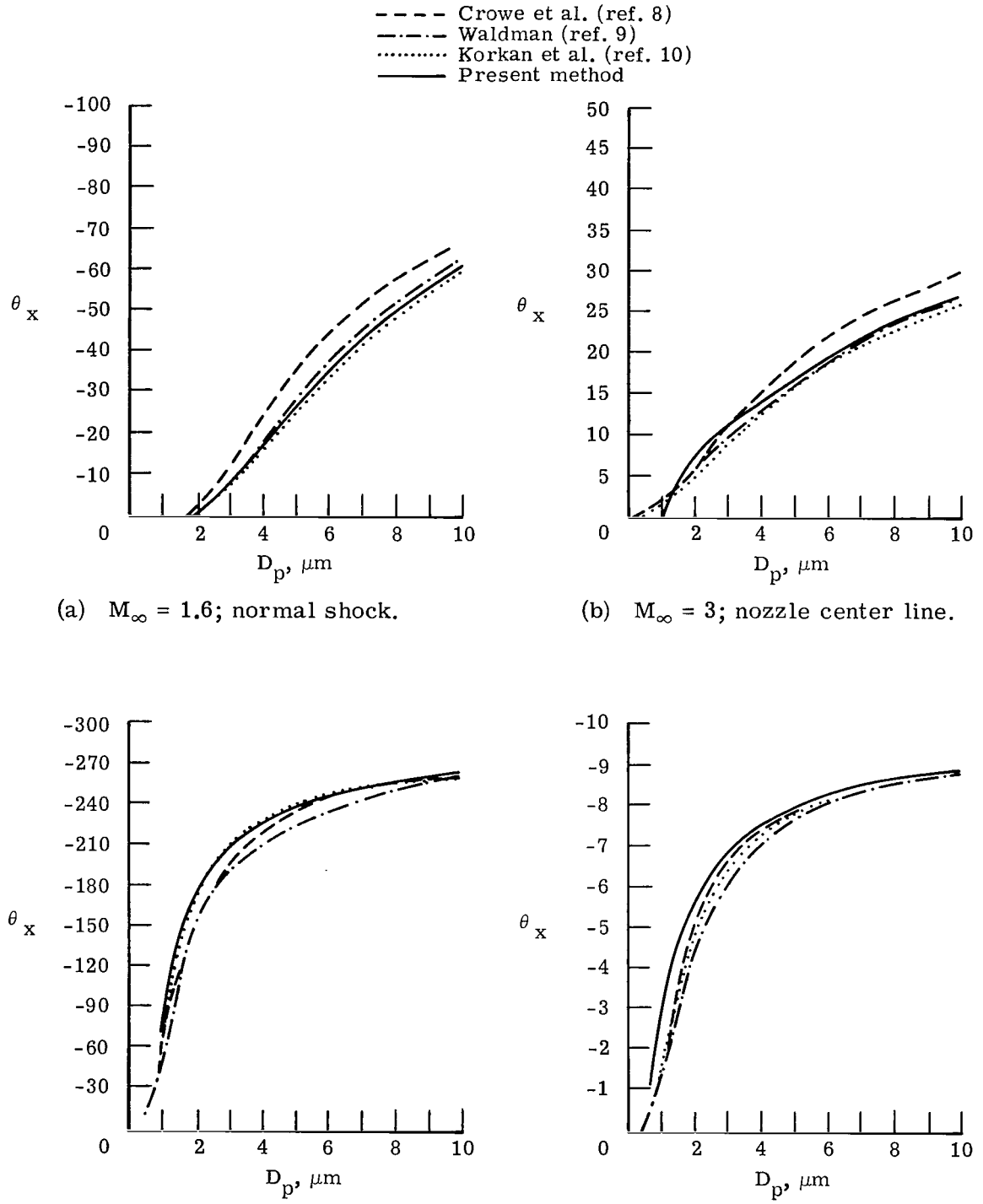

(a) $M_\infty = 1.6$; normal shock.

(b) $M_\infty = 3$; nozzle center line.

(c) $M_\infty = 3$; normal shock.

(d) $M_\infty = 3$; 10^o oblique shock x-component.

Figure 6.- At the points noted in table IV, percent velocity lag predicted by various methods.

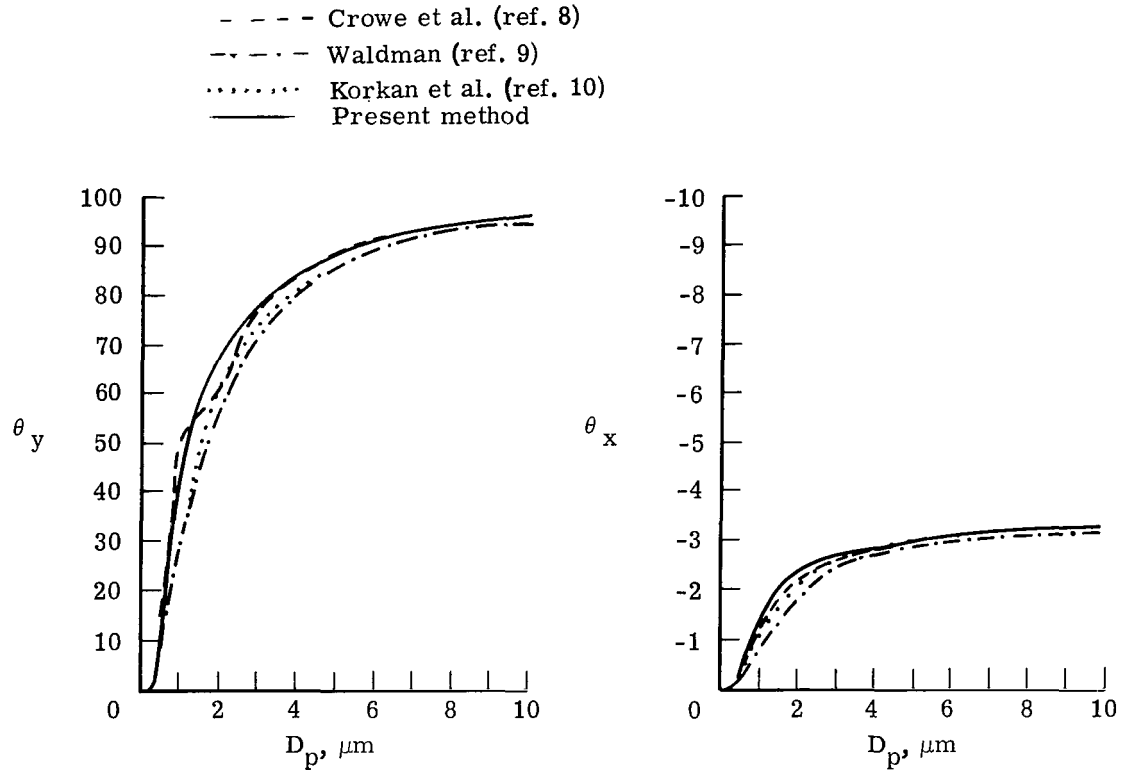

(e) $M_\infty = 3$; 10^o oblique shock y-component. (f) $M_\infty = 3$; 5^o oblique shock x-component.

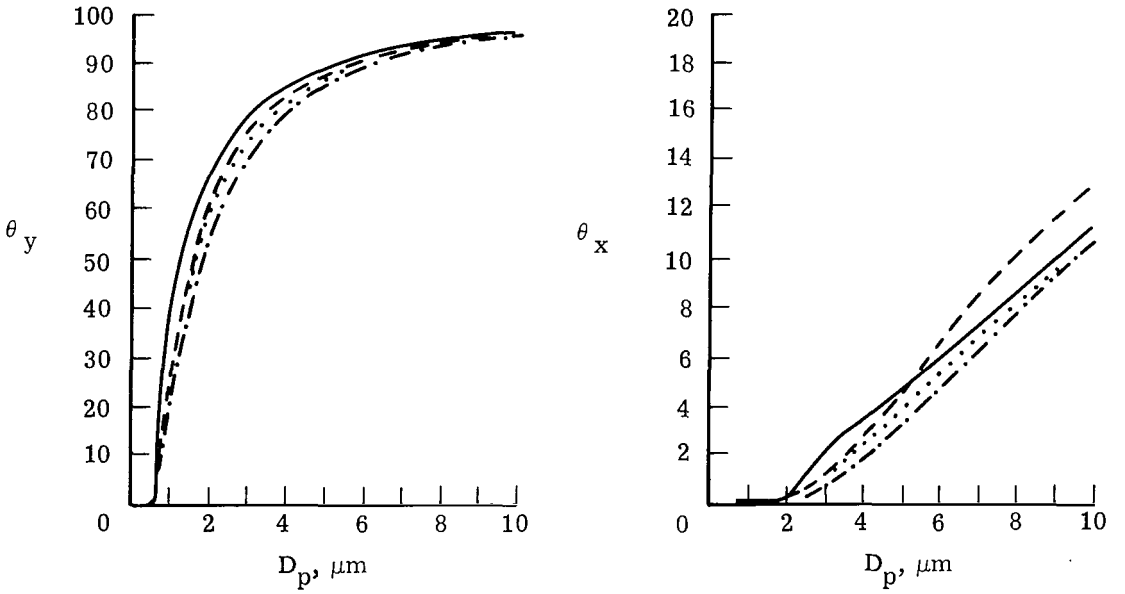

(g) $M_\infty = 3$; 5^o oblique shock y-component. (h) $M_\infty = 5$; nozzle center line.

Figure 6.- Continued.

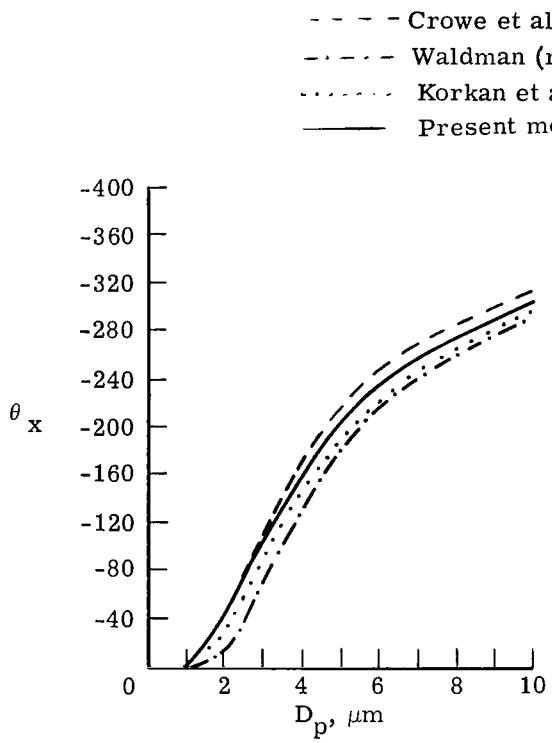

(i) $M_\infty = 5$; normal shock.

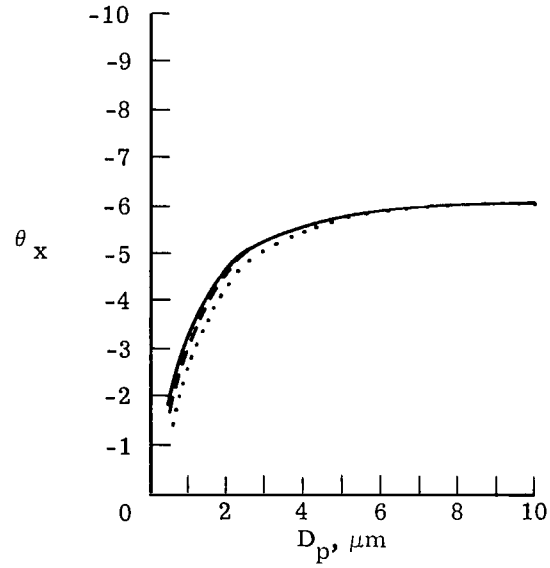

(j) $M_\infty = 5$; 10^o oblique shock x-component.

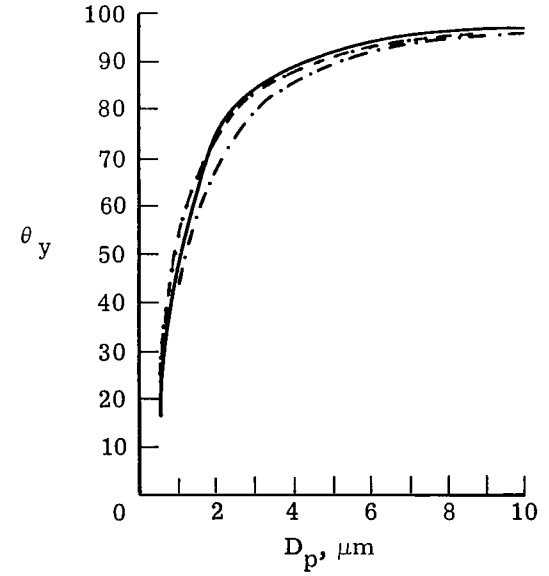

(k) $M_\infty = 5$; 10^o oblique shock y-component.

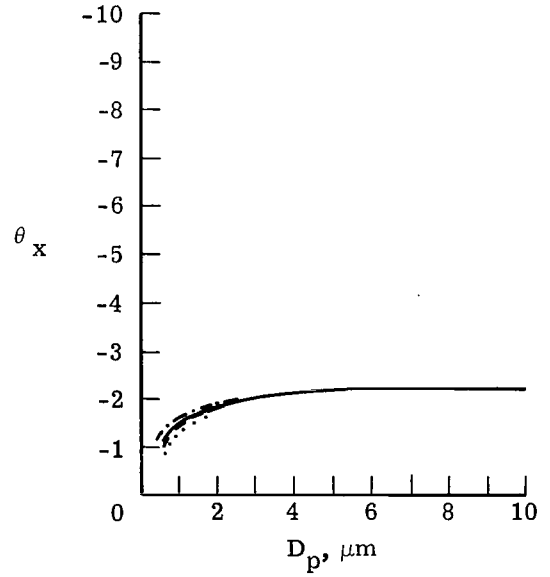

(l) $M_\infty = 5$; 5^o oblique shock x-component.

Figure 6.- Continued.

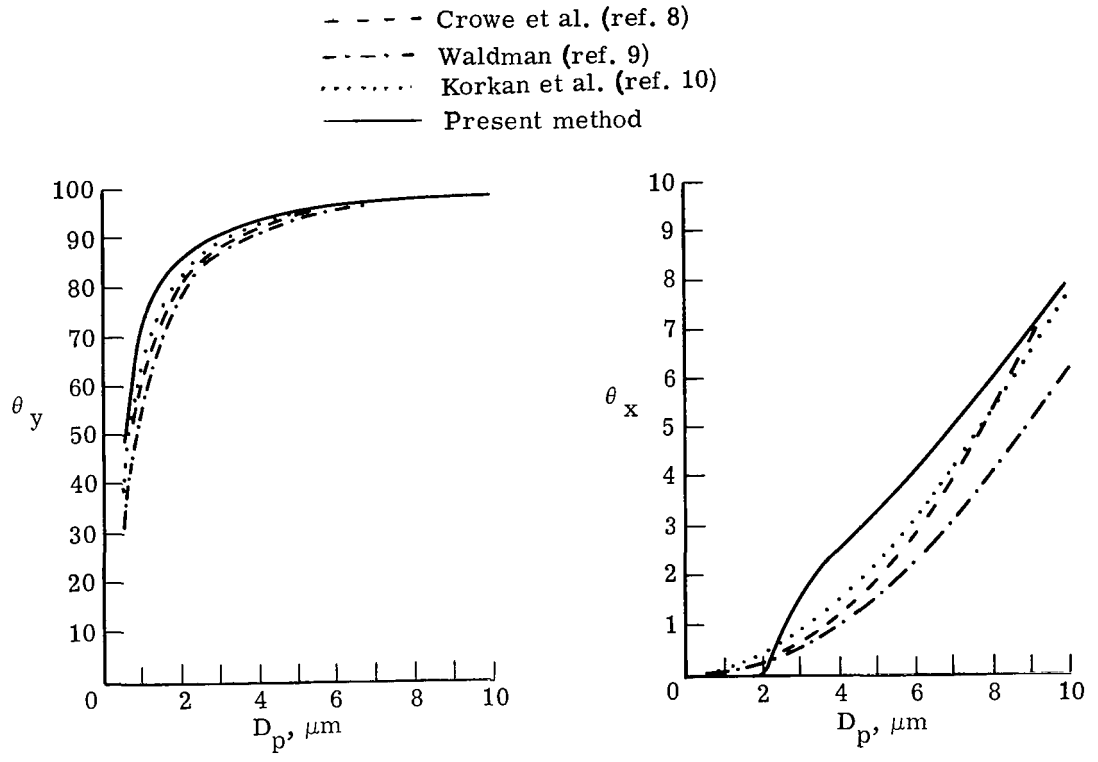

(m) $M_\infty = 5$; 5^o oblique shock y-component.

(n) $M_\infty = 6$; nozzle center line.

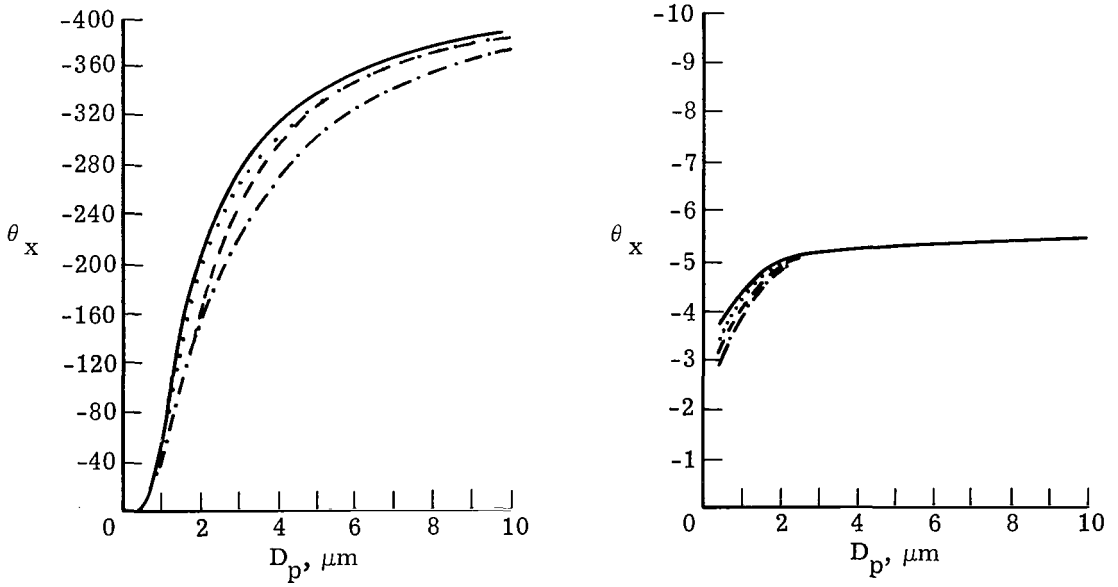

(o) $M_\infty = 6$; normal shock.

(p) $M_\infty = 6$; 10^o oblique shock x-component.

Figure 6.- Continued.

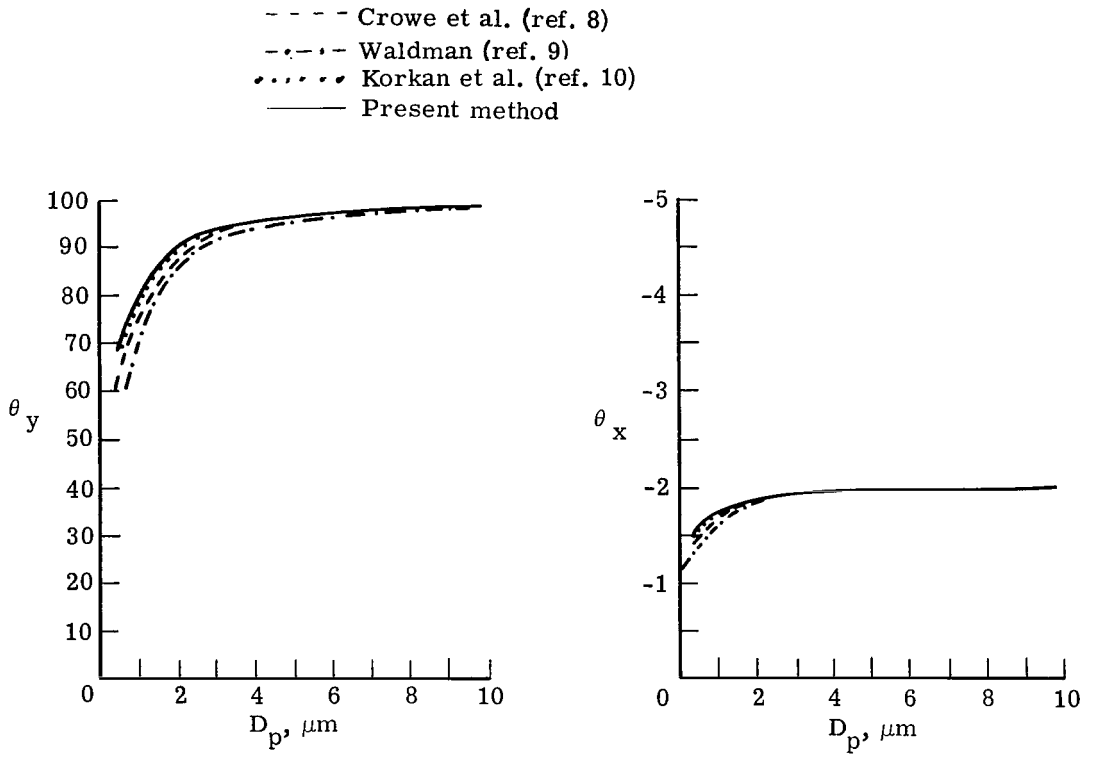

(q) $M_\infty = 6$; 10^o oblique shock y-component. (r) $M_\infty = 6$; 5^o oblique shock x-component.

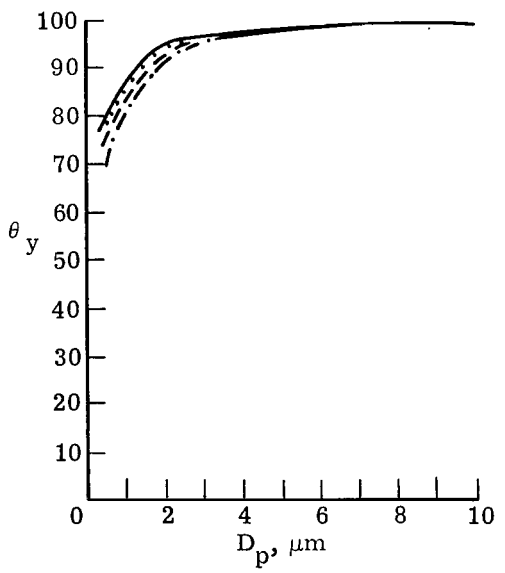

(s) $M_\infty = 6$; 5^o oblique shock y-component.

Figure 6.- Concluded.

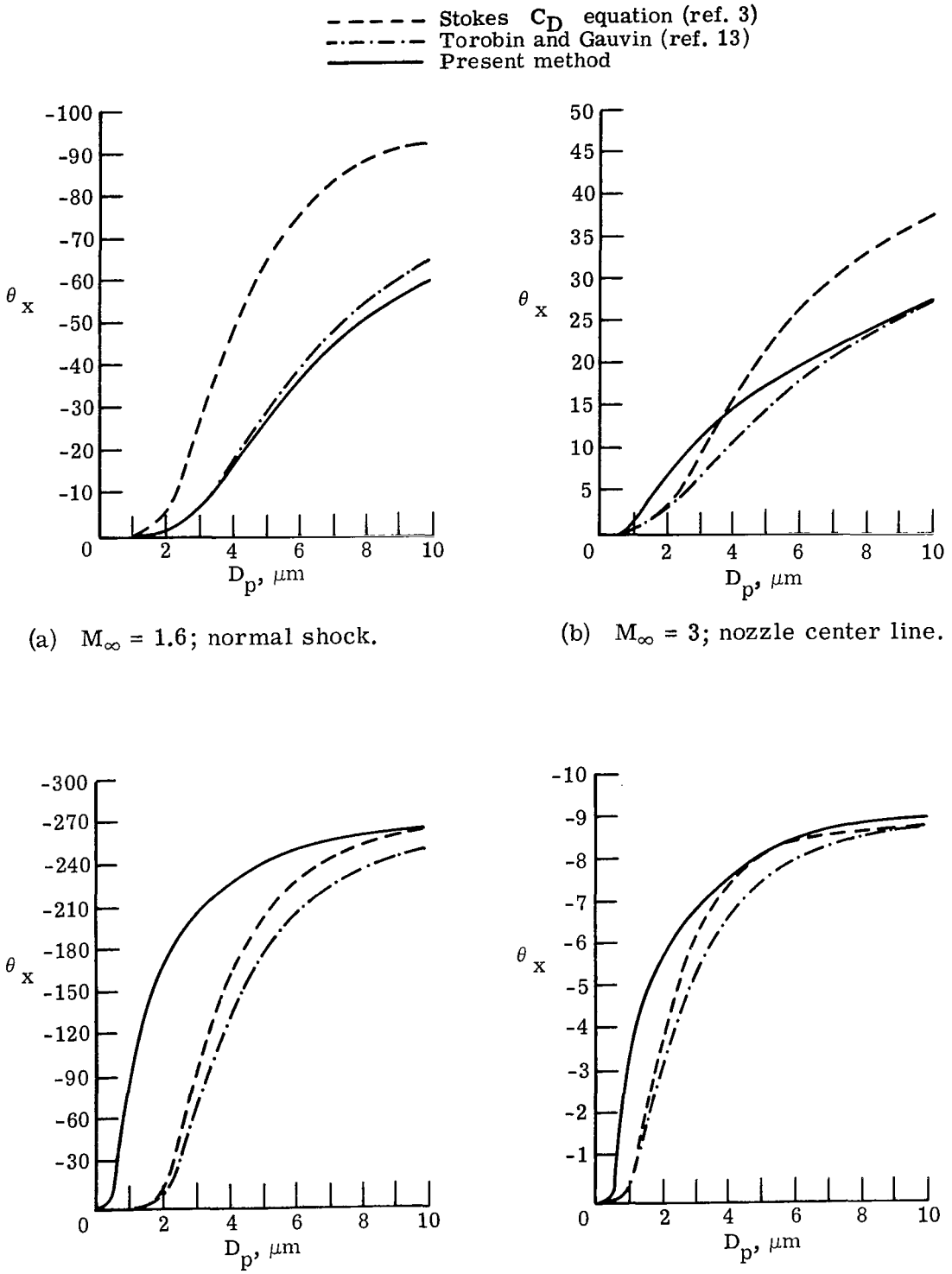

(a) $M_\infty = 1.6$; normal shock.

(b) $M_\infty = 3$; nozzle center line.

(c) $M_\infty = 3$; normal shock.

(d) $M_\infty = 3$; 10^o oblique shock x-component.

Figure 7.- At the points noted in table IV, percent velocity lag predicted by various methods.

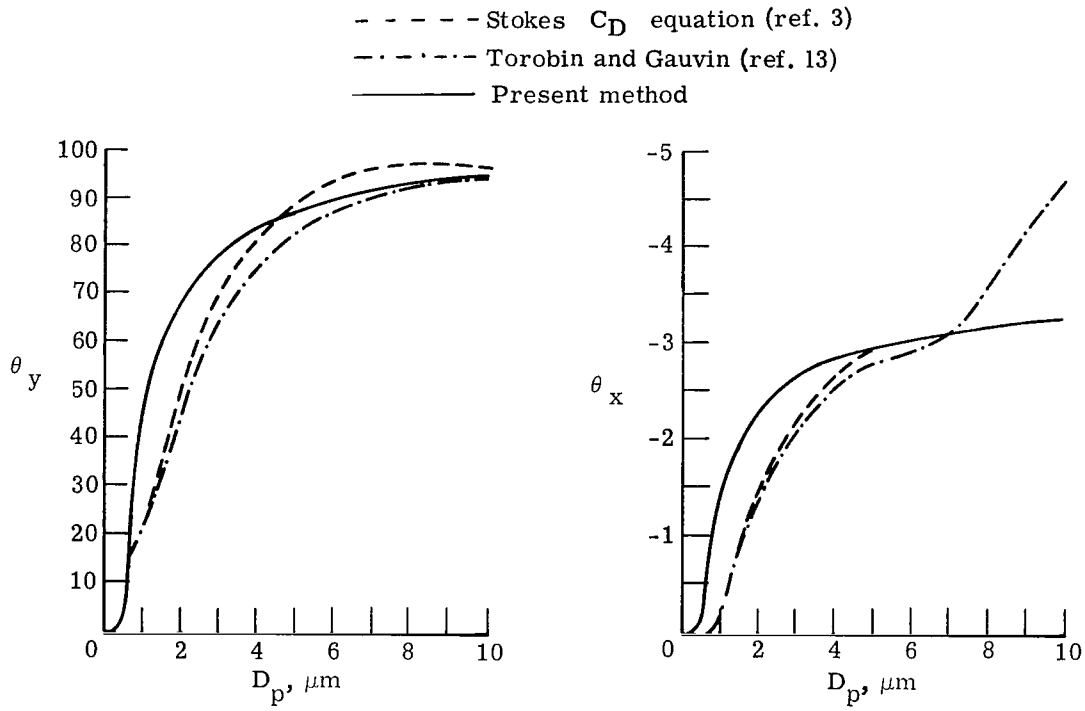

(e) $M_\infty = 3$; 10^o oblique shock y-component. (f) $M_\infty = 3$; 5^o oblique shock x-component.

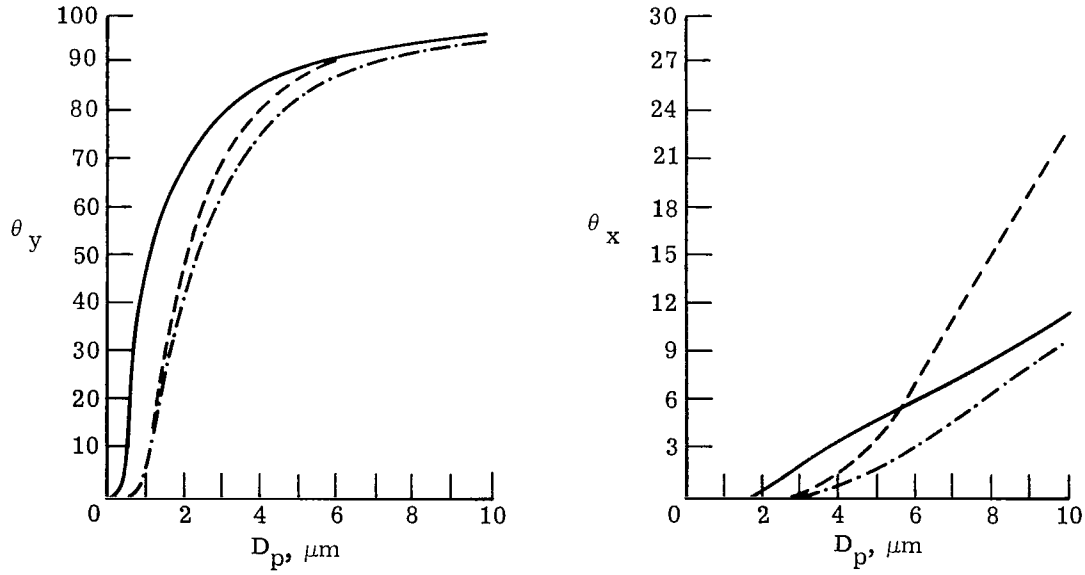

(g) $M_\infty = 3$; 5^o oblique shock y-component. (h) $M_\infty = 5$; nozzle center line.

Figure 7.- Continued.

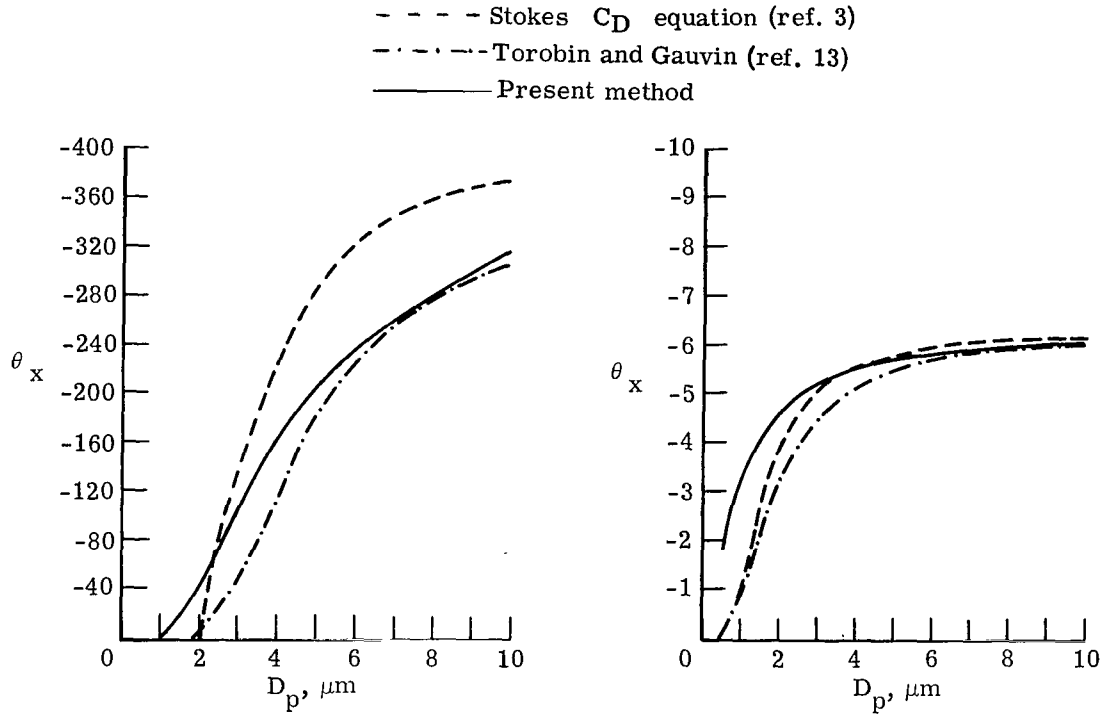

(i) $M_\infty = 5$; normal shock.

(j) $M_\infty = 5$; 10^o oblique shock x-component.

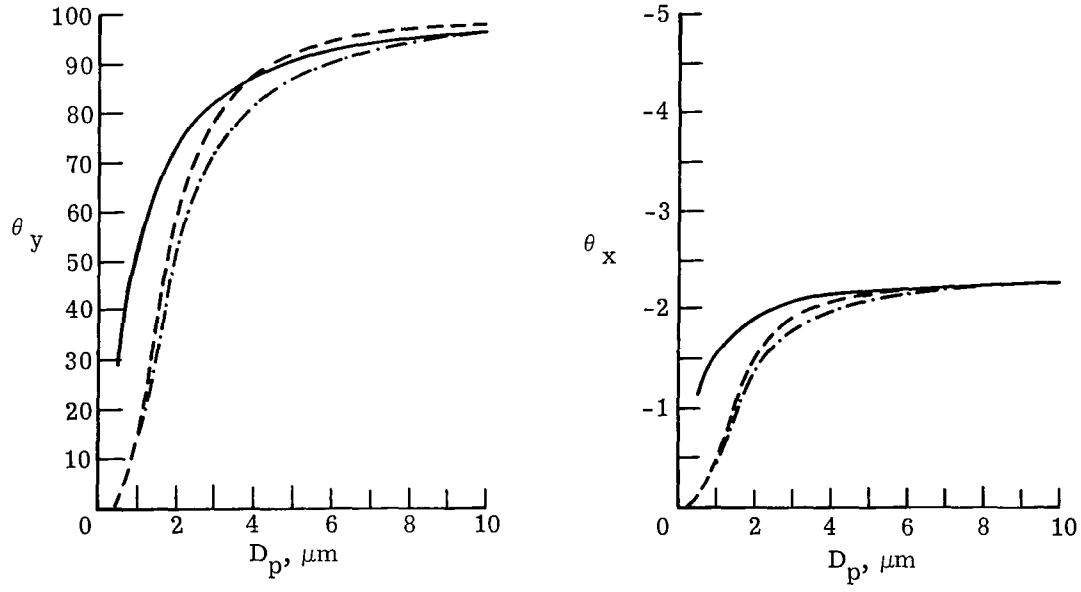

(k) $M_\infty = 5$; 10^o oblique shock y-component.

(l) $M_\infty = 5$; 5^o oblique shock x-component.

Figure 7.- Continued.

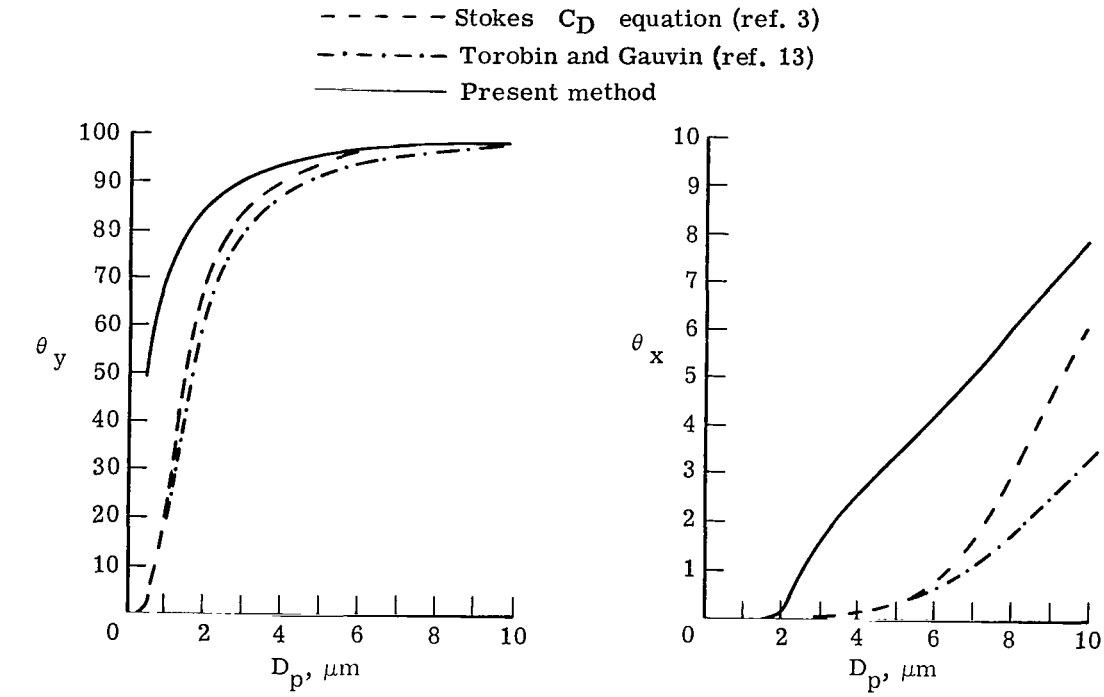

(m) $M_\infty = 5$; 5° oblique shock y-component.

(n) $M_\infty = 6$; nozzle center line.

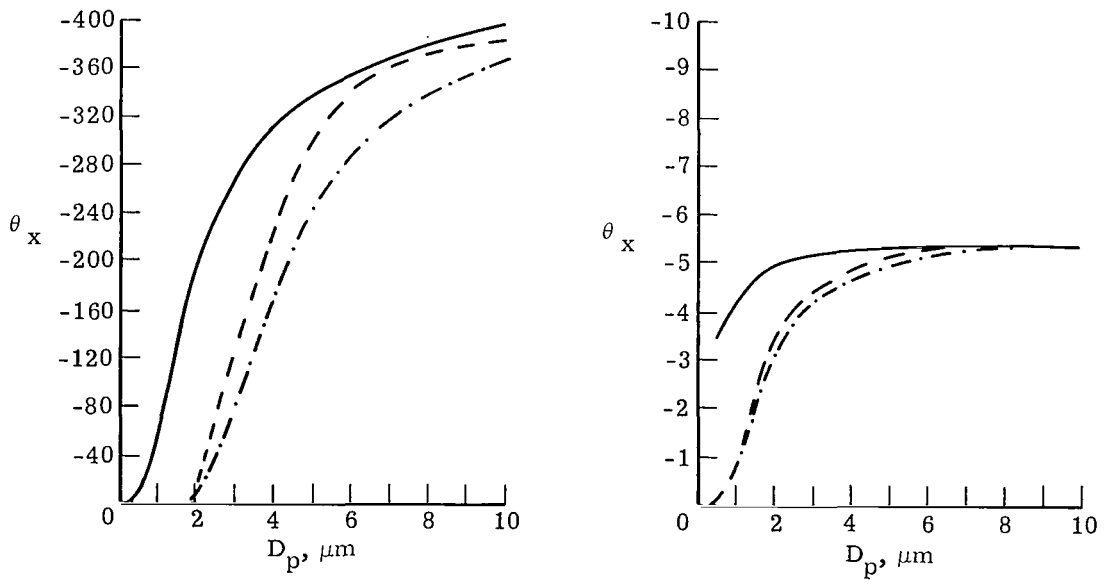

(o) $M_\infty = 6$; normal shock.

(p) $M_\infty = 6$; 10° oblique shock x-component.

Figure 7.- Continued.

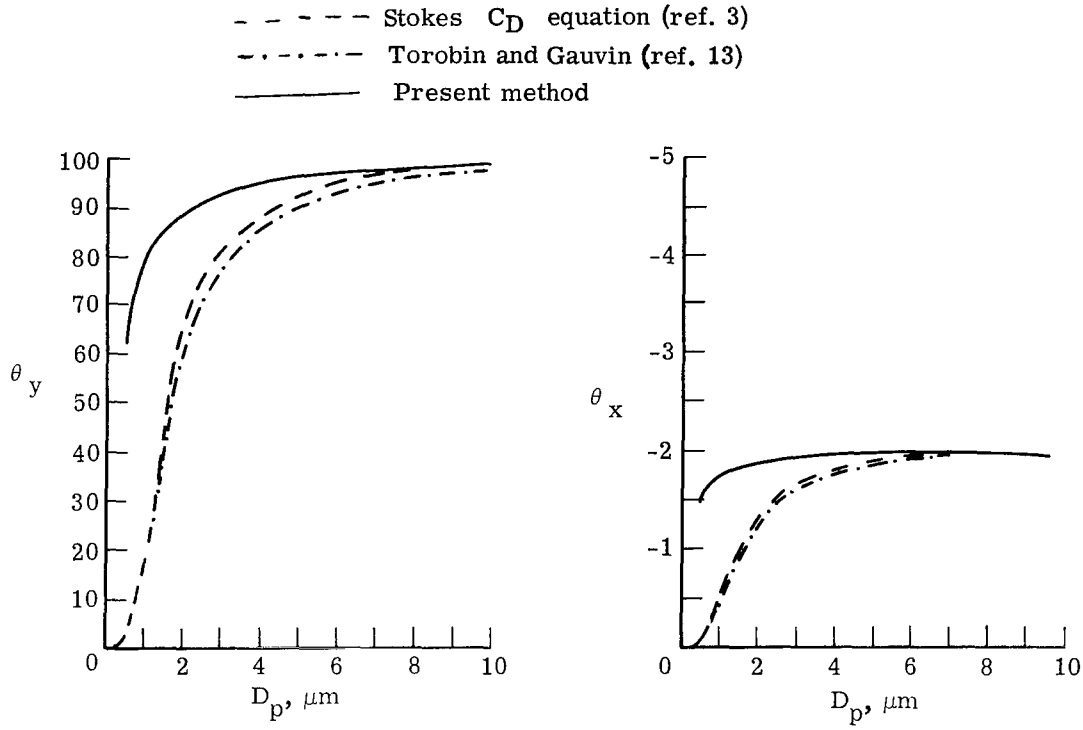

(q) $M_\infty = 6$; 10^o oblique shock y-component. (r) $M_\infty = 6$; 5^o oblique shock x-component.

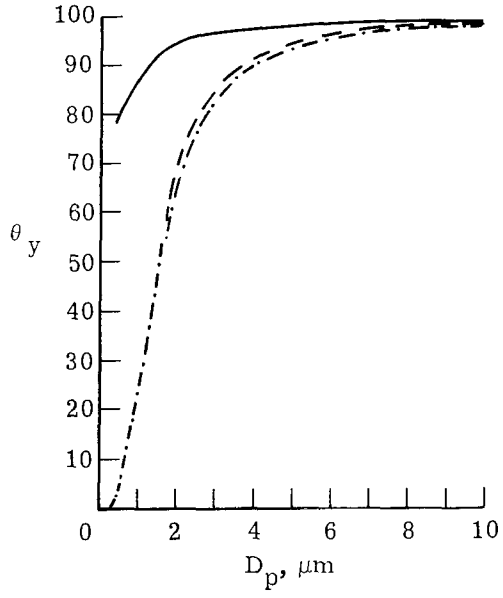

(s) $M_\infty = 6$; 5^o oblique shock y-component.

Figure 7.- Concluded.

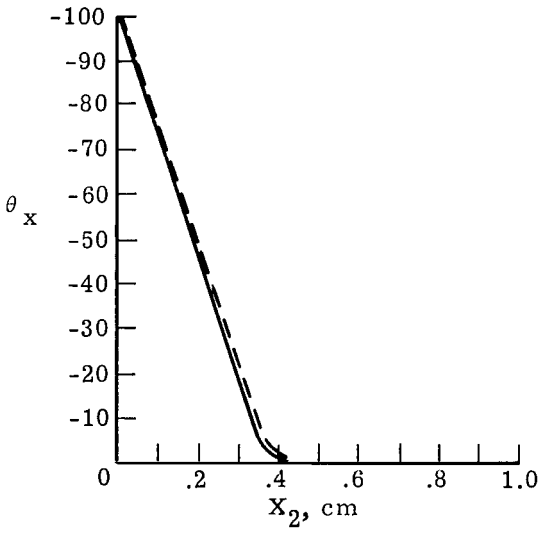

(a) Particle size, 1 μm.

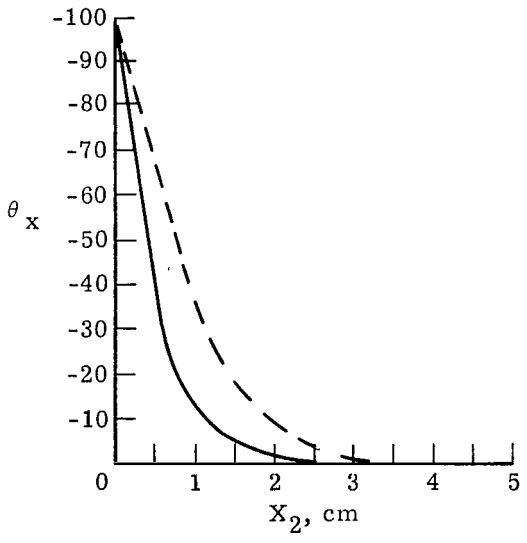

(b) Particle size, 3 μm.

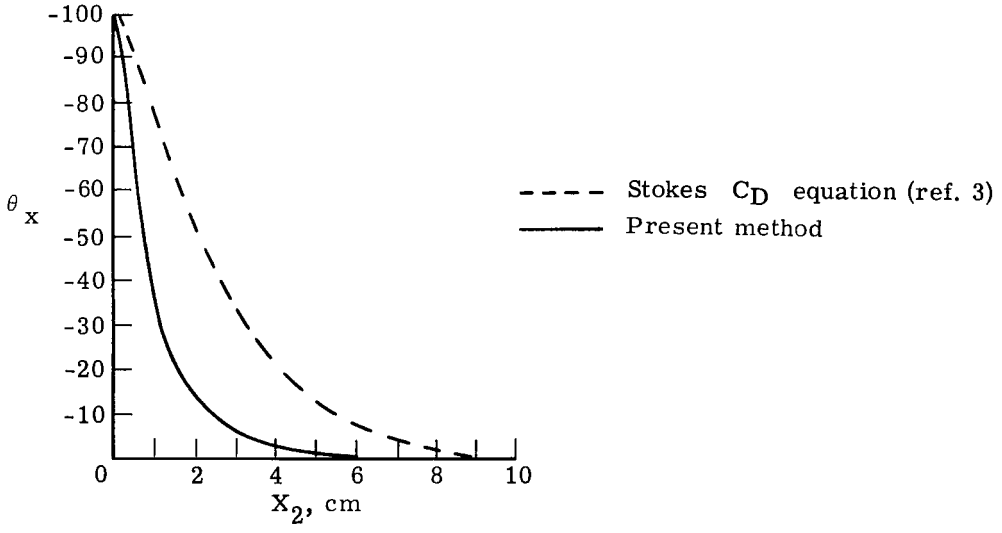

(c) Particle size, 5 μm.

Figure 8.- Variation of percent velocity lag behind a Mach 1.6 normal shock (stagnation conditions listed in table IV) predicted by various methods.

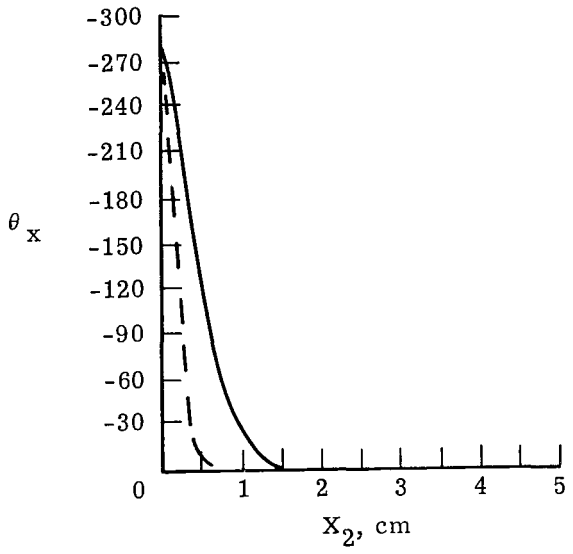

(a) Particle size, 1 μm.

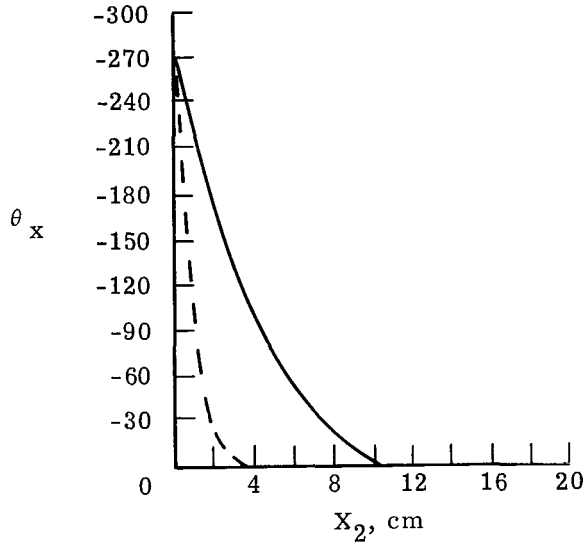

(b) Particle size, 3 μm.

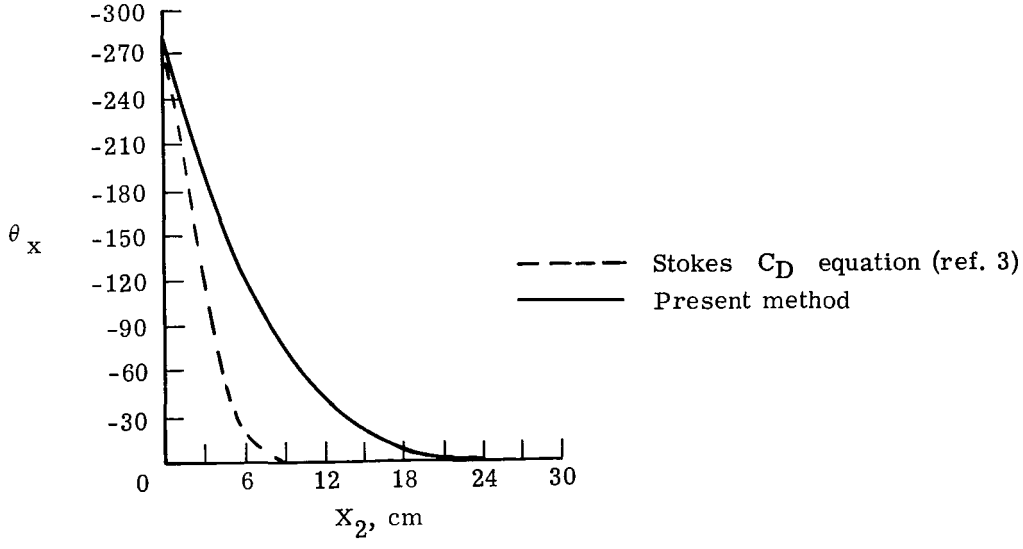

(c) Particle size, 5 μm.

Figure 9.- Variation of percent velocity lag behind a Mach 3 normal shock (stagnation conditions listed in table IV) predicted by two methods.

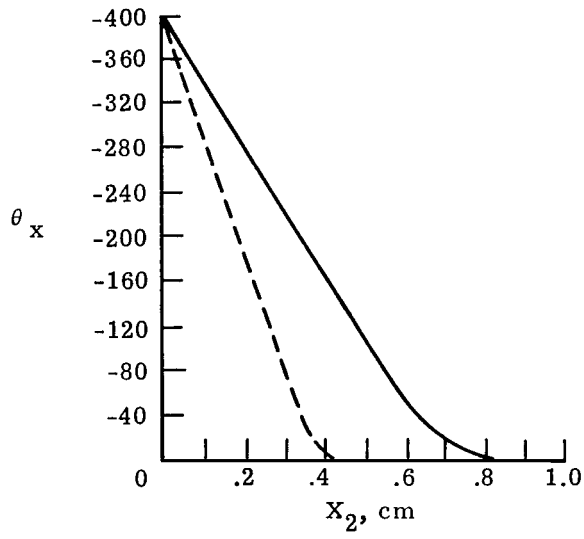

(a) Particle size, 1 μm.

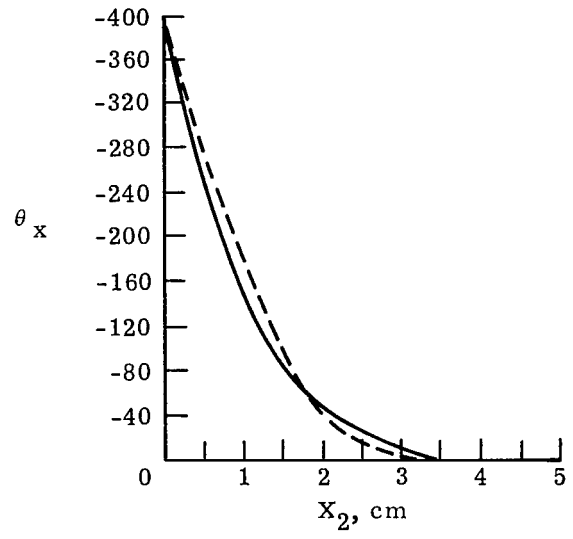

(b) Particle size, 3 μm.

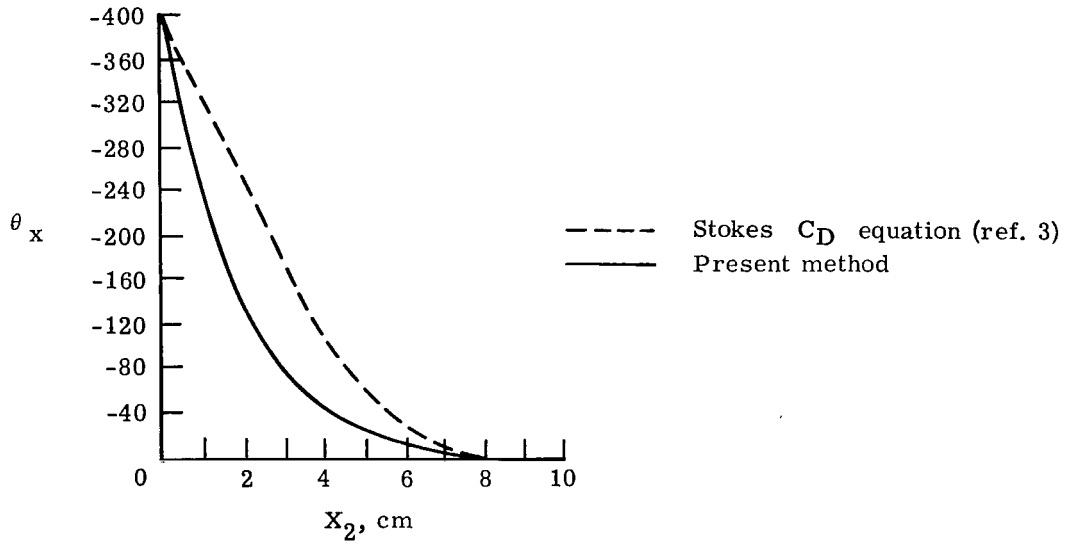

(c) Particle size, 5 μm.

Figure 10.- Variation of percent velocity lag behind a Mach 5 normal shock (stagnation conditions listed in table IV) predicted by two methods.

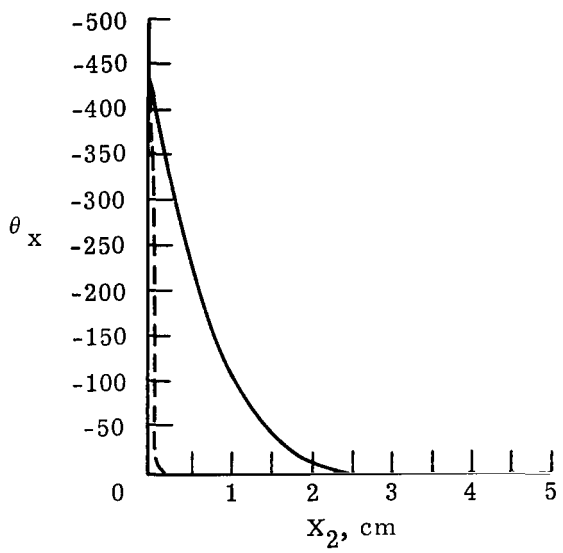

(a) Particle size, 1 μm.

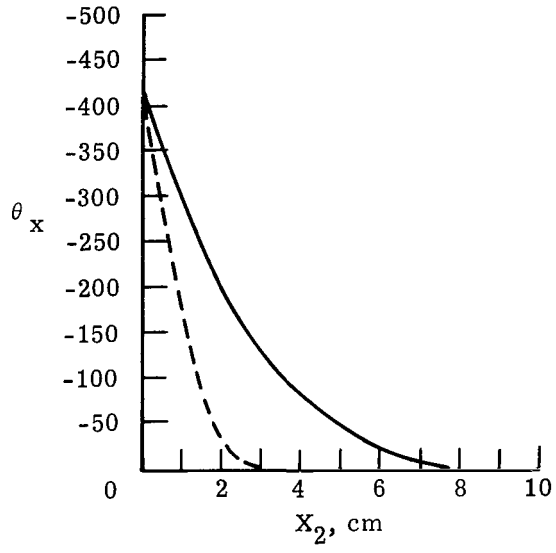

(b) Particle size, 3 μm.

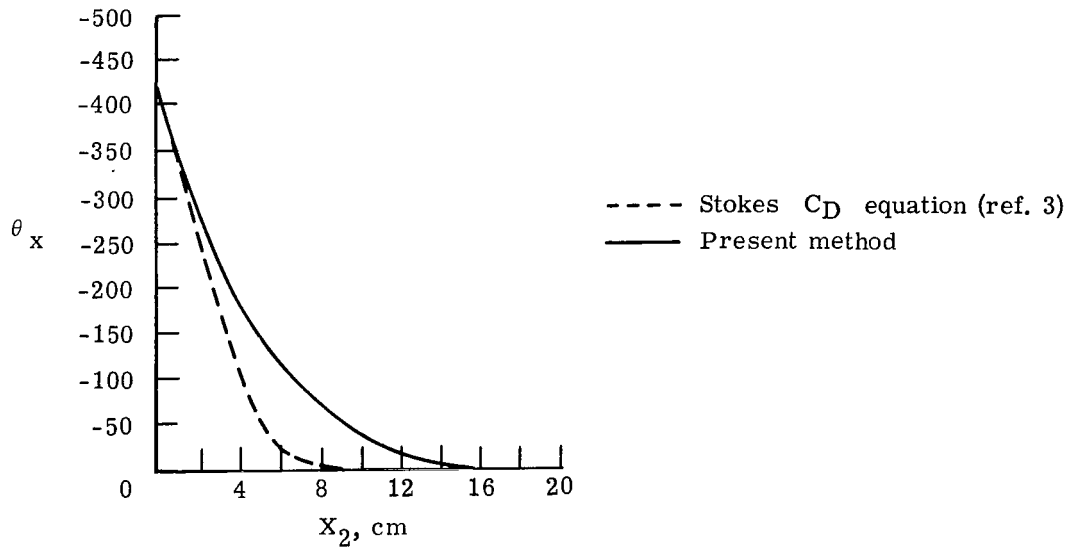

(c) Particle size, 5 μm.

Figure 11.- Variation of percent velocity lag behind a Mach 6 normal shock (stagnation conditions listed in table IV predicted by two methods.

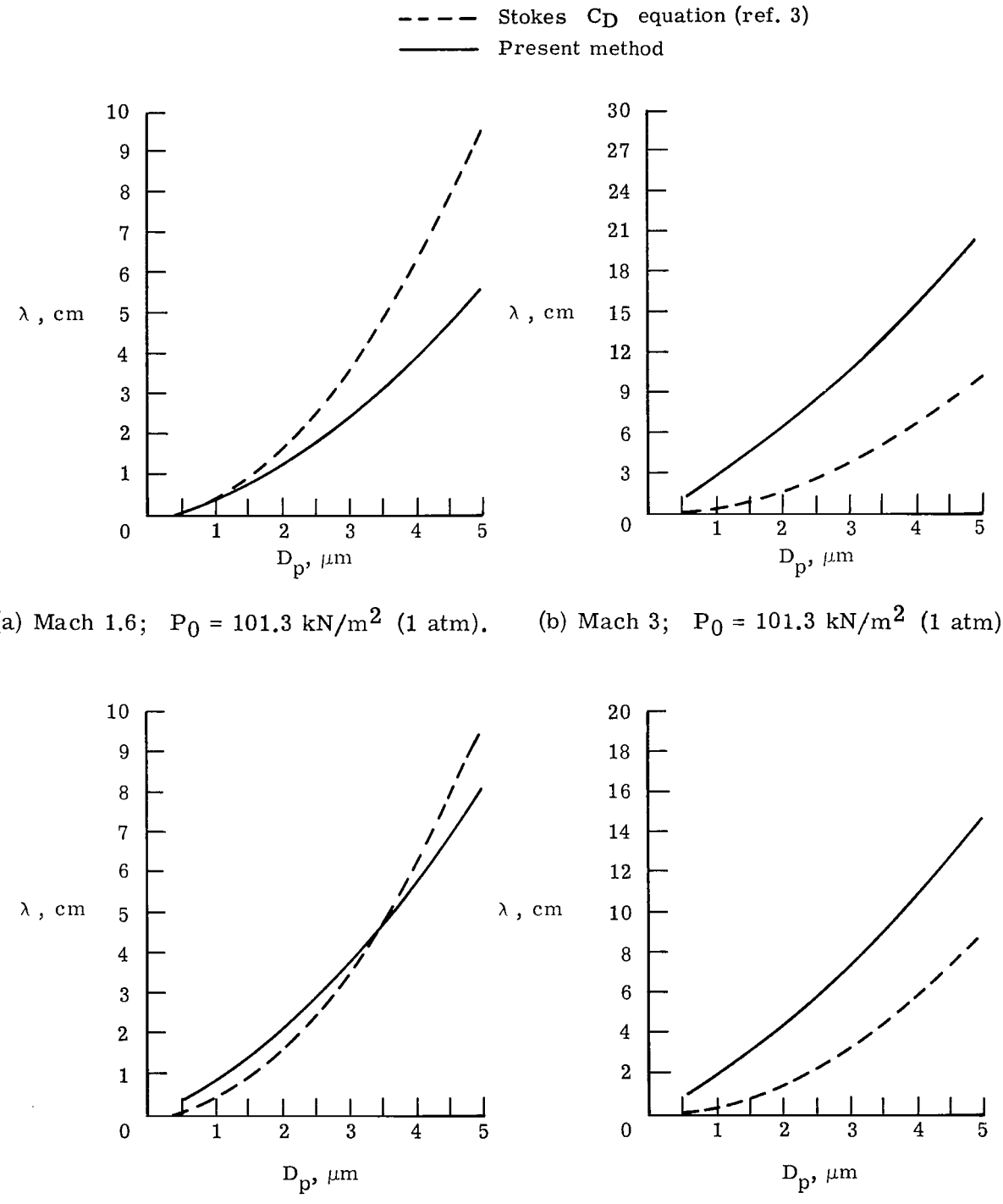

(a) Mach 1.6; P_0 = 101.3 kN/m^2 (1 atm).

(b) Mach 3; P_0 = 101.3 kN/m^2 (1 atm).

(c) Mach 5; P_0 = 344.6 kN/m^2 (3.4 atm).

(d) Mach 6; P_0 = 344.6 kN/m^2 (3.4 atm).

Figure 12.- Relaxation lengths behind normal shocks (stagnation conditions listed in table IV predicted by two methods.

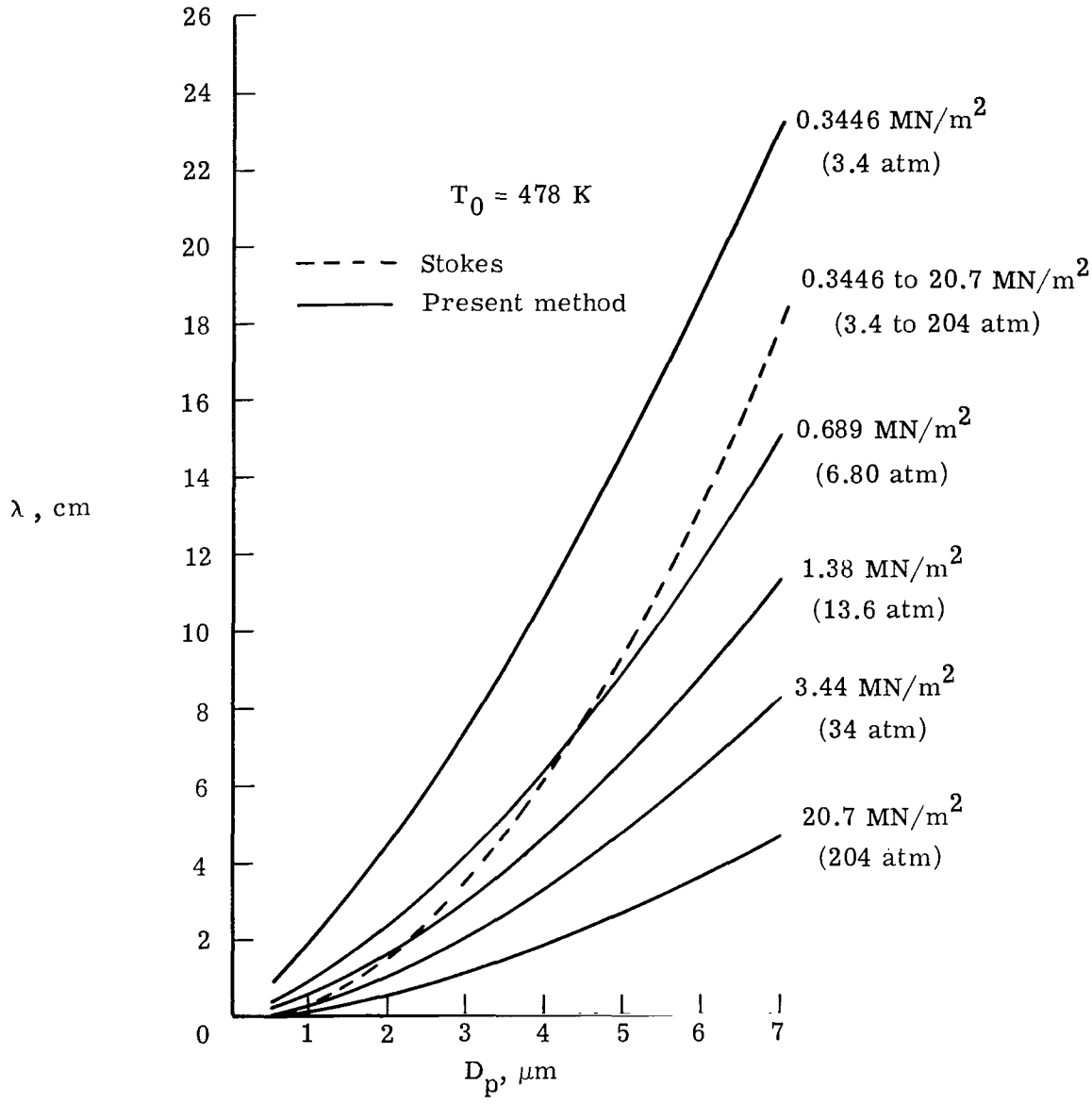

Figure 13.- Relaxation length behind a Mach 6 normal shock as a function of stagnation pressure.

NASA-Langley, 1976 L-10258

265 001 C1 U D 760130 S00903DS
DEPT OF THE AIR FORCE
AF WEAPONS LABORATORY
ATTN: TECHNICAL LIBRARY (SUL)
KIRTLAND AFB NM 87117

"The aeronautical and space activities of the United States shall be conducted so as to contribute . . . to the expansion of human knowledge of phenomena in the atmosphere and space. The Administration shall provide for the widest practicable and appropriate dissemination of information concerning its activities and the results thereof."

—NATIONAL AERONAUTICS AND SPACE ACT OF 1958

NASA SCIENTIFIC AND TECHNICAL PUBLICATIONS

TECHNICAL REPORTS: Scientific and technical information considered important, complete, and a lasting contribution to existing knowledge.

TECHNICAL NOTES: Information less broad in scope but nevertheless of importance as a contribution to existing knowledge.

TECHNICAL MEMORANDUMS: Information receiving limited distribution because of preliminary data, security classification, or other reasons. Also includes conference proceedings with either limited or unlimited distribution.

CONTRACTOR REPORTS: Scientific and technical information generated under a NASA contract or grant and considered an important contribution to existing knowledge.

TECHNICAL TRANSLATIONS: Information published in a foreign language considered to merit NASA distribution in English.

SPECIAL PUBLICATIONS: Information derived from or of value to NASA activities. Publications include final reports of major projects, monographs, data compilations, handbooks, sourcebooks, and special bibliographies.

TECHNOLOGY UTILIZATION PUBLICATIONS: Information on technology used by NASA that may be of particular interest in commercial and other non-aerospace applications. Publications include Tech Briefs, Technology Utilization Reports and Technology Surveys.

Details on the availability of these publications may be obtained from:

SCIENTIFIC AND TECHNICAL INFORMATION OFFICE

NATIONAL AERONAUTICS AND SPACE ADMINISTRATION

Washington, D.C. 20546